
NIST SPECIAL PUBLICATION 260-130

U.S. DEPARTMENT OF COMMERCE/Technology Administration
National Institute of Standards and Technology

*Standard Reference Materials:*

# Glass Fiberboard, SRM 1450c, for Thermal Resistance from 280 K to 340 K

Robert R. Zarr

# NIST Special Publication 260-130

*Standard Reference Materials:*

# Glass Fiberboard, SRM 1450c, for Thermal Resistance from 280 K to 340 K

Robert R. Zarr

Building and Fire Research Laboratory
National Institute of Standards and Technology
Gaithersburg, MD 20899-0001


U.S. DEPARTMENT OF COMMERCE, William M. Daley, Secretary
TECHNOLOGY ADMINISTRATION, Mary L. Good, Under Secretary for Technology
NATIONAL INSTITUTE OF STANDARDS AND TECHNOLOGY, Arati Prabhakar, Director

Issued April 1997

**National Institute of Standards and Technology Special Publication 260–130**
**Natl. Inst. Stand. Technol. Spec. Publ. 260–130, 64 pages (April 1997)**
**CODEN: NSPUE2**

**U.S. GOVERNMENT PRINTING OFFICE**
**WASHINGTON: 1997**

For sale by the Superintendent of Documents, U.S. Government Printing Office, Washington, DC 20402–9325

## Foreword

Since its inauguration in 1901, the National Institute of Standards and Technology (NIST), formerly the National Bureau of Standards (NBS), has issued nearly 2000 different Standard Samples or Standard Reference Materials © (SRMs). Many of these have been renewed several times; others have been replaced or discontinued as technology changed. Today, over 1000 SRMs are available, together with a large number of scientific publications related to the fundamental and applied characteristics of these materials. Each material is certified for chemical composition, chemical properties, or its physical or mechanical characteristics. Each SRM is provided with a Certificate or a Certificate of Analysis that contains the essential data concerning its properties or characteristics. The SRMs currently available cover a wide range of chemical, physical, and mechanical properties, and a corresponding wide range of measurement interests in practically all aspects of fundamental and applied science. These SRMs constitute a unique and invaluable means of transferring to the user accurate data obtained at NIST, and provide essential tools that can be used to improve accuracy in practically all areas where measurements are performed.

In addition to SRMs, NIST issues a variety of Reference Materials (RMs) which are sold, but not certified, by NIST. They meet the International Standards Organization (ISO) Guide 30-1981 (E) definition for RMs, and many meet the ISO definition for Certified Reference Materials (CRMs). The documentation issued with these materials is either (1) a "Report of Investigation," or (2) a "Certificate," issued by the certifying agency (other than NIST), e.g., other national laboratories, other government agencies, other standardizing bodies, or other non-profit organizations. Reference Materials are intended to further scientific or technical research on particular materials. The principal consideration in issuing RMs is to provide a homogeneous material so that investigators in different laboratories are assured that they are investigating the same material. When deemed to be in the public interest and when alternate means of national distribution do not exist, NIST acts as the distributor for such materials.

Further information on the reference materials available from NIST may be obtained from the Standard Reference Materials Program, National Institute of Standards and Technology, Gaithersburg, MD 20899. Information on other NIST services may be obtained from Technology Services, National Institute of Standards and Technology, Gaithersburg, MD 20899. NIST provides a number of additional services, that include: Calibration and Related Measurement Services, National Standard Reference Data, Accreditation of Testing Laboratories, National Center for Standards and Certification Information, Weights and Measures Program and Proficiency Sample Programs.

## Preface

Standard Reference Materials (SRMs) as defined by the National Institute of Standards and Technology (NIST) are well-characterized materials, produced in quantity and certified for one or more physical or chemical properties. They are used to assure the accuracy and compatibility of measurements throughout the nation. SRMs are widely used as primary standards in many diverse fields in science, industry, and technology, both within the United States and throughout the world. They are also used extensively in the fields of environmental and clinical analysis. In many applications, traceability of quality control and measurement processes to the national measurement system is carried out through the mechanism and use of SRMs. For many of the Nation's scientists and technologists, it is therefore of more than passing interest to know the details of the measurements made at NIST in arriving at the certified values of the SRMs produced. The NIST Special Publication 260 Series is a series of papers reserved for this purpose.

The 260 Series is dedicated to the dissemination of information on different phases of the preparation, measurement, certification, and use of NIST SRMs. In general, much more detail will be found in these papers than is generally allowed, or desirable, in scientific journal articles. This enables the user to assess the validity and accuracy of the measurement processes employed, to judge the statistical analysis, and to learn details of techniques and methods utilized for work entailing greatest care and accuracy. These papers also should provide sufficient additional information so SRMs can be utilized in new applications in diverse fields not foreseen at the time the SRM was originally issued.

Inquiries concerning the technical content of this paper should be directed to the author(s). Other questions concerned with the availability, delivery, price, and so forth, will receive prompt attention from:

Standard Reference Materials Program
Building 202, Room 204
National Institute of Standards and Technology
Gaithersburg, MD 20899
Telephone: (301) 975-6776
FAX: (301) 948-3730

Thomas E. Gills, Chief
Standard Reference Materials Program

## Abstract

Thermal conductivity measurements at room temperature are presented as the basis for certified values of thermal resistance for SRM 1450c, Fibrous Glass Board. The measurements have been conducted in accordance with a randomized full factorial experimental design with two variables, bulk density and temperature, using NIST's one-meter line-heat-source guarded-hot-plate apparatus. Uncertainties of the measurements, consistent in format with current international guidelines, have been prepared. The thermal conductivity was measured over ranges of bulk density from 150 $kg/m^3$ to 165 $kg/m^3$ and mean temperature from 280 K to 340 K. Statistical analyses of the physical properties from the SRM are presented and include variations between boards, as well as within board. Material characterization, including the material's microstructure, is presented. Results are compared to data from previous material lots of the SRM 1450 Series as well as to data from an international round robin of guarded-hot-plate apparatus.



## Keywords

building technology; calibration; density; fibrous glass board; guarded hot plate; heat flow meter; interlaboratory; round robin; standard reference material (SRM) 1450; thermal conductivity; thermal insulation; uncertainty

## OTHER NIST PUBLICATIONS IN THIS SERIES


Trahey, N.M., ed., NIST Standard Reference Materials Catalog 1995-96, NIST Spec. Publ. 260 (1995 Ed.). PB95-232518/AS*

Michaelis, R.E., and Wyman, L.L., Standard Reference Materials: Preparation of White Cast Iron Spectrochemical Standards, NBS Misc. Publ. 260-1 (June 1964). COM74-11061**

Michaelis, R.E., Wyman, L.L., and Flitsch, R., Standard Reference Materials: Preparation of NBS Copper-Base Spectrochemical Standards, NBS Misc. Publ. 260-2 (October 1964). COM74-11063**

Michaelis, R.E., Yakowitz, H., and Moore, G.A., Standard Reference Materials: Metallographic Characterization of an NBS Spectrometric Low-Alloy Steel Standard, NBS Misc. Publ. 260-3 (October 1964). COM74-11060**

Hague, J.L., Mears, T.W., and Michaelis, R.E., Standard Reference Materials: Sources of Information, Publ. 260-4 (February 1965). COM74-11059**

Alvarez, R., and Flitsch, R., Standard Reference Materials: Accuracy of Solution X-Ray Spectrometric Analysis of Copper-Base Alloys, NBS Misc. Publ. 260-5 (February 1965). PB168068**

Shultz, J.I., Standard Reference Materials: Methods for the Chemical Analysis of White Cast Iron Standards, NBS Misc. Publ. 260-6 (July 1965). COM74-11068**

Bell, R.K., Standard Reference Materials: Methods for the Chemical Analysis of NBS Copper-Base Spectrochemical Standards, NBS Misc. Publ. 260-7 (October 1965). COM74-11067**

Richmond, M.S., Standard Reference Materials: Analysis of Uranium Concentrates at the National Bureau of Standards, NBS Misc. Publ. 260-8 (December 1965). COM74-11066**

Anspach, S.C., Cavallo, L.M., Garfinkel, S.B., et al., Standard Reference Materials: Half Lives of Materials Used in the Preparation of Standard Reference Materials of Nineteen Radioactive Nuclides Issued by the National Bureau of Standards, NBS Misc. Publ. 260-9 (November 1965). COM74-11065**

Yakowitz, H., Vieth, D.L., Heinrich, K.F.J., et al., Standard Reference Materials: Homogeneity Characterization of NBS Spectrometric Standards II: Cartridge Brass and Low-Alloy Steel, NBS Misc. Publ. 260-10 (December 1965). COM74-11064**

Napolitano, A., and Hawkins, E.G., Standard Reference Materials: Viscosity of Standard Lead-Silica Glass, NBS Misc. Publ. 260-11** (November 1966).

Yakowitz, H., Vieth, D.L., and Michaelis, R.E., Standard Reference Materials: Homogeneity Characterization of NBS Spectrometric Standards III: White Cast Iron and Stainless Steel Powder Compact, NBS Misc. Publ. 260-12 (September 1966).

Spijkerman, J.J., Snediker, D.K., Ruegg, F.C., et al., Standard Reference Materials: Mossbauer Spectroscopy Standard for the Chemical Shift of Iron Compounds, NBS Misc. Publ. 260-13** (July 1967).

Menis, O., and Sterling, J.T., Standard Reference Materials: Determination of Oxygen in Ferrous Materials (SRMs 1090, 1091, 1092), NBS Misc. Publ. 260-14** (September 1966).

Passaglia, E. and Shouse, P.J., Standard Reference Materials: Recommended Method of Use of Standard Light-Sensitive Paper for Calibrating Carbon Arcs Used in Testing Testiles for Colorfastness to Light, NBS Spec. Publ. 260-15 (July 1967). Superseded by SP 260-41.

Yakowitz, H., Michaelis, R.E., and Vieth, D.L., Standard Reference Materials: Homogeneity Characterization of NBS Spectrometric Standards IV: Preparation and Microprobe Characterization of W-20% Mo Alloy Fabricated by Powder Metallurgical Methods, NBS Spec. Publ. 260-16 (January 1969). COM74-11062**

Catanzaro, E.J., Champion, C.E., Garner, E.L., et al., Standard Reference Materials: Boric Acid; Isotopic, and Assay Standard Reference Materials, NBS Spec. Publ. 260-17 (February 1970). PB189457**

Geller, S.B., Mantek, P.A., and Cleveland, N.G., Calibration of NBS Secondary Standards Magnetic Tape Computer Amplitude Reference Amplitude Measurement "Process A," NBS Spec. Publ. 260-18 (November 1969). Superseded by SP 260-29.

Paule, R.C., and Mandel, J., Standard Reference Materials: Analysis of Interlaboratory Measurements on the Vapor Pressure of Gold (Certification of SRM 745). NBS Spec. Publ. 260-19 (January 1970). PB190071**

260-20: Unassigned

Paule, R.C., and Mandel, J., Standard Reference Materials: Analysis of Interlaboratory Measurements on the Vapor Pressures of Cadmium and Silver, NBS Spec. Publ. 260-21 (January 1971). COM74-11359**

Yakowitz, H., Fiori, C.E., and Michaelis, R.E., Standard Reference Materials: Homogeneity Characterization of Fe-3 Si Alloy, NBS Spec. Publ. 260-22 (February 1971). COM74-11357**

Napolitano, A., and Hawkins, E.G., Standard Reference Materials: Viscosity of a Standard Borosilicate Glass, NBS Spec. Publ. 260-23 (December 1970). COM71-00157**

Sappenfield, K.M., Marinenko, G., and Hague, J.L., Standard Reference Materials: Comparison of Redox Standards, NBS Spec. Publ. 260-24 (January 1972). COM72-50058**

Hicho, G.E., Yakowitz, H., Rasberry, S.D., et al., Standard Reference Materials: A Standard Reference Material Containing Nominally Four Percent Austenite, NBS Spec. Publ. 260-25 (February 1971). COM74-11356**

Martin, J.F., Standard Reference Materials: NBS-U.S. Steel Corp. Joint Program for Determining Oxygen and Nitrogen in Steel, NBS Spec. Publ. 260-26 (February 1971). PB 81176620**

Garner, E.L., Machlan, L.A., and Shields, W.R., Standard Reference Materials: Uranium Isotopic Standard Reference Materials, NBS Spec. Publ. 260-27 (April 1971). COM74-11358**

Heinrich, K.F.J., Myklebust, R.L., Rasberry, S.D., et al., Standard Reference Materials: Preparation and Evaluation of SRMs 481 and 482 Gold-Silver and Gold-Copper Alloys for Microanalysis, NBS Spec. Publ. 260-28 (August 1971). COM71-50365**

Geller, S.B., Standard Reference Materials: Calibration of NBS Secondary Standard Magnetic Tape (Computer Amplitude Reference) Using the Reference Tape Amplitude Measurement "Process A-Model 2," NBS Spec. Publ. 260-29 (June 1971). COM71-50282** Supersedes Measurement System in SP 260-18.

Gorozhanina, R.S., Freedman, A.Y., and Shaievitch, A.B., (translated by M.C. Selby), Standard Reference Materials: Standard Samples Issued in the USSR (A Translation from the Russian), NBS Spec. Publ. 260-30 (June 1971). COM71-50283**

Hust, J.G., and Sparks, L.L., Standard Reference Materials: Thermal Conductivity of Electrolytic Iron SRM 734 from 4 to300 K, NBS Spec. Publ. 260-31 (November 1971). COM71-50563**

Mavrodineanu, R., and Lazar, J.W., Standard Reference Materials: Standard Quartz Cuvettes for High Accuracy Spectrophotometry, NBS Spec. Publ. 260-32 (December 1973). COM74-50018**

Wagner, H.L., Standard Reference Materials: Comparison of Original and Supplemental SRM 705, Narrow Molecular Weight Distribution Polystyrene, NBS Spec. Publ. 260-33 (May 1972). COM72-50526**

Sparks, L.L., and Hust, J.G., Standard Reference Material: Thermoelectric Voltage of Silver-28 Atomic Percent Gold Thermocouple Wire, SRM 733, Verses Common Thermocouple Materials (Between Liquid Helium and Ice Fixed Points), NBS Spec. Publ. 260-34 (April 1972). COM72-50371**

Sparks, L.L., and Hust, J.G., Standard Reference Materials: Thermal Conductivity of Austenitic Stainless Steel, SRM 735 from 5 to 280 K, NBS Spec. Publ. 260-35 (April 1972). COM72-50368**

Cali, J.P., Mandel, J., Moore, L.J., et al., Standard Reference Materials: A Reference Method for the Determination of Calcium in Serum NBS SRM 915, NBS Spec. Publ. 260-36 (May 1972). COM72-50527**

Shultz, J.I., Bell, R.K., Rains, T.C., et al., Standard Reference Materials: Methods of Analysis of NBS Clay Standards, NBS Spec. Publ. 260-37 (June 1972). COM72-50692**

Richard, J.C., and Hsia, J.J., Standard Reference Materials: Preparation and Calibration of Standards of Spectral Specular Reflectance, NBS Spec. Publ. 260-38 (May 1972). COM72-50528**

Clark, A.F., Denson, V.A., Hust, J.G., et al., Standard Reference Materials: The Eddy Current Decay Method for Resistivity Characterization of High-Purity Metals, NBS Spec. Publ. 260-39 (May 1972). COM72-50529**

McAdie, H.G., Garn, P.D., and Menis, O., Standard Reference Materials: Selection of Differential Thermal Analysis Temperature Standards Through a Cooperative Study (SRMs 758, 759, 760), NBS Spec. Publ. 260-40 (August 1972) COM72-50776**

Wood. L.A., and Shouse, P.J., Standard Reference Materials: Use of Standard Light-Sensitive Paper for Calibrating Carbon Arcs Used in Testing Textiles for Colorfastness to Light, NBS Spec. Publ. 260-41 (August 1972). COM72-50775**

Wagner, H.L., and Verdier, P.H., eds., Standard Reference Materials: The Characterization of Linear Polyethylene, SRM 1475, NBS Spec. Publ. 260-42 (September 1972). COM72-50944**

Yakowitz, H., Ruff, A.W., and Michaelis, R.E., Standard Reference Materials: Preparation and Homogeneity Characterization of an Austenitic Iron-Chromium-Nickel Alloy, NBS Spec. Publ. 260-43 (November 1972). COM73-50760**

Schooley, J.F., Soulen, R.J., Jr., and Evans, G.A., Jr., Standard Reference Materials: Preparation and Use of Superconductive Fixed Point Devices, SRM 767, NBS Spec. Publ. 260-44 (December 1972). COM73-50037**

Greifer, B., Maienthal, E.J., Rains, T.C., et al., Standard Reference Materials: Development of NBS SRM 1579 Powdered Lead-Based Paint, NBS Spec. Publ. 260-45 (March 1973). COM73-50226**

Hust, J.G., and Giarratano, P.J., Standard Reference Materials: Thermal Conductivity and Electrical Resistivity Standard Reference Materials: Austenitic Stainless Steel, SRMs 735 and 798, from 4 to 1200 K, NBS Spec. Publ. 260-46 (March 1975). COM75-10339**

Hust, J.G., Standard Reference Materials: Electrical Resistivity of Electrolytic Iron, SRM 797, and Austenitic Stainless Steel, SRM 798, from 5 to 280 K, NBS Spec. Publ. 260-47 (February 1974). COM74-50176**

Mangum, B.W., and Wise, J.A., Standard Reference Materials: Description and Use of Precision Thermometers for the Clinical Laboratory, SRM 933 and SRM 934, NBS Spec. Publ. 260-48 (May 1974). Superseded by NIST Spec. Publ. 260-113. COM74-50533**

Carpenter, B.S., and Reimer, G.M., Standard Reference Materials: Calibrated Glass Standards for Fission Track Use, NBS Spec. Publ. 260-49 (November 1974). COM74-51185**

Hust, J.G., and Giarratano, P.J., Standard Reference Materials: Thermal Conductivity and Electrical Resistivity Standard Reference Materials: Electrolytic Iron, SRMs 734 and 797 from 4 to 1000 K, NBS Spec. Publ. 260-50 (June 1975). COM75-10698**

Mavrodineanu, R., and Baldwin, J.R., Standard Reference Materials: Glass Filters As a SRM for Spectrophotometry-Selection, Preparation, Certification, and Use-SRM 930 NBS Spec. Publ. 260-51 (November 1975). COM75-10339**

Hust, J.G., and Giarratano, P.J., Standard Reference Materials: Thermal Conductivity and Electrical Resistivity SRMs 730 and 799, from 4 to 3000 K, NBS Spec. Publ. 260-52 (September 1975). COM75-11193**

Durst, R.A., Standard Reference Materials: Standardization of pH Measurements, NBS Spec. Publ. 260-53 (December 1978). Superseded by SP 260-53 Rev. 1988 Edition. PB88217427**

Burke, R.W., and Mavrodineanu, R., Standard Reference Materials: Certification and Use of Acidic Potassium Dichromate Solutions as an Ultraviolet Absorbance Standard, NBS Spec. Publ. 260-54 (August 1977). PB272168**

Ditmars, D.A., Cezairliyan, A., Ishihara, S., et al., Standard Reference Materials: Enthalpy and Heat Capacity; Molybdenum SRM 781, from 273 to 2800 K, NBS Spec. Publ. 260-55 (September 1977). PB272127**

Powell, R.L., Sparks, L.L., and Hust, J.G., Standard Reference Materials: Standard Thermocouple Material, Pt-67: SRM 1967, NBS Spec. Publ. 260-56 (February 1978). PB277172**

Cali, J.P., and Plebanski, T., Standard Reference Materials: Guide to United States Reference Materials, NBS Spec. Publ. 260-57 (February 1978). PB277173**

Barnes, J.D., and Martin, G.M., Standard Reference Materials: Polyester Film for Oxygen Gas Transmission Measurements SRM 1470, NBS Spec. Publ. 260-58 (June 1979). PB297098**

Chang, T., and Kahn, A.H., Standard Reference Materials: Electron Paramagnetic Resonance Intensity Standard: SRM 2601; Description and Use, NBS Spec. Publ. 260-59 (August 1978). PB292097**

Velapoldi, R.A., Paule, R.C., Schaffer, R., et al., Standard Reference Materials: A Reference Method for the Determination of Sodium in Serum, NBS Spec. Publ. 260-60 (August 1978). PB286944**

Verdier, P.H., and Wagner, H.L., Standard Reference Materials: The Characterization of Linear Polyethylene (SRMs 1482, 1483, 1484), NBS Spec. Publ. 260-61 (December 1978). PB289899**

Soulen, R.J., and Dove, R.B., Standard Reference Materials: Temperature Reference Standard for Use Below 0.5 K (SRM 768), NBS Spec. Publ. 260-62 (April 1979). PB294245**

Velapoldi, R.A., Paule, R.C., Schaffer, R., et al., Standard Reference Materials: A Reference Method for the Determination of Potassium in Serum, NBS Spec. Publ. 260-63 (May 1979). PB297207**

Velapoldi, R.A., and Mielenz, K.D., Standard Reference Materials: A Fluorescence SRM Quinine Sulfate Dihydrate (SRM 936), NBS Spec. Publ. 260-64 (January 1980). PB80132046**

Marinenko, R.B., Heinrich, K.F.J., and Ruegg, F.C., Standard Reference Materials: Micro-Homogeneity Studies of NBS SRM, NBS Research Materials, and Other Related Samples, NBS Spec. Publ. 260-65 (September 1979). PB300461**

Venable, W.H., Jr., and Eckerle, K.L., Standard Reference Materials: Didymium Glass Filters for Calibrating the Wavelength Scale of Spectrophotometers (SRMs 2009, 2010, 2013, 2014). NBS Spec. Publ. 260-66 (October 1979). PB80104961**

Velapoldi, R.A., Paule, R.C., Schaffer, R., et al., Standard Reference Materials: A Reference Method for the Determination of Chloride in Serum, NBS Spec. Publ. 260-67 (November 1979). PB80110117**

Mavrodineanu, R., and Baldwin, J.R., Standard Reference Materials: Metal-On-Quartz Filters as a SRM for Spectrophotometry SRM 2031, NBS Spec. Publ. 260-68 (April 1980). PB80197486**

Velapoldi, R.A., Paule, R.C., Schaffer, R., et al., Standard Reference Materials: A Reference Method for the Determination of Lithium in Serum, NBS Spec. Publ. 260-69 (July 1980). PB80209117**

Marinenko, R.B., Biancaniello, F., Boyer, P.A., et al., Standard Reference Materials: Preparation and Characterization of an Iron-Chromium-Nickel Alloy for Microanalysis: SRM 479a, NBS Spec. Publ. 260-70 (May 1981). SN003-003-02328-1*

Seward, R.W., and Mavrodineanu, R., Standard Reference Materials: Summary of the Clinical Laboratory Standards Issued by the National Bureau of Standards, NBS Spec. Publ. 260-71 (November 1981). PB82135161**

Reeder, D.J., Coxon, B., Enagonio, D., et al., Standard Reference Materials: SRM 900, Anti-epilepsy Drug Level Assay Standard, NBS Spec. Publ. 260-72 (June 1981). PB81220758

Interrante, C.G., and Hicho, G.E., Standard Reference Materials: A Standard Reference Material Containing Nominally Fifteen Percent Austenite (SRM 486), NBS Spec. Publ. 260-73 (January 1982). PB82215559**

Marinenko, R.B., Standard Reference Materials: Preparation and Characterization of K-411 and K-412 Mineral Glasses for Microanalysis: SRM 470, NBS Spec. Publ. 260-74 (April 1982). PB82221300**

Weidner, V.R., and Hsia, J.J., Standard Reference Materials: Preparation and Calibration of First Surface Aluminum Mirror Specular Reflectance Standards (SRM 2003a), NBS Spec. Publ. 260-75 (May 1982). PB82221367**

Hicho, G.E., and Eaton, E.E., Standard Reference Materials: A Standard Reference Material Containing Nominally Five Percent Austenite (SRM 485a), NBS Spec. Publ. 260-76 (August 1982). PB83115568**

Furukawa, G.T., Riddle, J.L., Bigge, W.G., et al., Standard Reference Materials: Application of Some Metal SRMs as Thermometric Fixed Points, NBS Spec. Publ. 260-77 (August 1982). PB83117325**

Hicho, G.E., and Eaton, E.E., Standard Reference Materials: Standard Reference Material Containing Nominally Thirty Percent Austenite (SRM 487), NBS Spec. Publ. 260-78 (September 1982). PB83115576**

Richmond, J.C., Hsia, J.J., Weidner, V.R., et al., Standard Reference Materials: Second Surface Mirror Standards of Specular Spectral Reflectance (SRMs 2023, 2024, 2025), NBS Spec. Publ. 260-79 (October 1982). PB84203447**

Schaffer, R., Mandel, J., Sun, T., et al., Standard Reference Materials: Evaluation by an ID/MS Method of the AACC Reference Method for Serum Glucose, NBS Spec. Publ. 260-80 (October 1982). PB84216894**

Burke, R.W., and Mavrodineanu, R., Standard Reference Materials: Accuracy in Analytical Spectrophotometry, NBS Spec. Publ. 260-81 (April 1983). PB83214536**

Weidner, V.R., Standard Reference Materials: White Opal Glass Diffuse Spectral Reflectance Standards for the Visible Spectrum (SRMs 2015 and 2016), NBS Spec. Publ. 260-82 (April 1983). PB83220723**

Bowers, G.N., Jr., Alvarez, R., Cali, J.P., et al., Standard Reference Materials: The Measurement of the Catalytic (Activity) Concentration of Seven Enzymes in NBS Human Serum (SRM 909), NBS Spec. Publ. 260-83 (June 1983). PB83239509**

Gills, T.E., Seward, R.W., Collins, R.J., et al., Standard Reference Materials: Sampling, Materials Handling, Processing, and Packaging of NBS Sulfur in Coal SRMs 2682, 2683, 2684, and 2685, NBS Spec. Publ. 260-84 (August 1983). PB84109552**

Swyt, D.A., Standard Reference Materials: A Look at Techniques for the Dimensional Calibration of Standard Microscopic Particles, NBS Spec. Publ. 260-85 (September 1983). PB84112648**

Hicho, G.E., and Eaton, E.E., Standard Reference Materials: A SRM Containing Two and One-Half Percent Austenite, SRM 488, NBS Spec. Publ. 260-86 (December 1983). PB84143296**

Mangum, B.W., Standard Reference Materials: SRM 1969: Rubidium Triple-Point - A Temperature Reference Standard Near 39.30° C, NBS Spec. Publ. 260-87 (December 1983). PB84149996**

Gladney, E.S., Burns, C.E., Perrin, D.R., et al., Standard Reference Materials: 1982 Compilation of Elemental Concentration Data for NBS Biological, Geological, and Environmental Standard Reference Materials, NBS Spec. Publ. 260-88 (March 1984). PB84218338**

Hust, J.G., Standard Reference Materials: A Fine-Grained, Isotropic Graphite for Use as NBS Thermophysical Property RMs from 5 to 2500 K, NBS Spec. Publ. 260-89 (September 1984). PB85112886**

Hust, J.G., and Lankford, A.B., Standard Reference Materials: Update of Thermal Conductivity and Electrical Resistivity of Electrolytic Iron, Tungsten, and Stainless Steel, NBS Spec. Publ. 260-90 (September 1984). PB85115814**

Goodrich, L.F., Vecchia, D.F., Pittman, E.S., et al., Standard Reference Materials: Critical Current Measurements on an NbTi Superconducting Wire SRM, NBS Spec. Publ. 260-91 (September 1984). PB85118594**

Carpenter, B.S., Standard Reference Materials: Calibrated Glass Standards for Fission Track Use (Supplement to NBS Spec. Publ. 260-49), NBS Spec. Publ. 260-92 (September 1984). PB85113025**

Ehrstein, J.R., Standard Reference Materials: Preparation and Certification of SRM for Calibration of Spreading Resistance Probes, NBS Spec. Publ. 260-93 (January 1985). PB85177921**

Gills, T.E., Koch, W.F., Stolz, J.W., et al., Standard Reference Materials: Methods and Procedures Used at the National Bureau of Standards to Certify Sulfur in Coal SRMs for Sulfur Content, Calorific Value, Ash Content, NBS Spec. Publ. 260-94 (December 1984). PB85165900**

Mulholland, G.W., Hartman, A.W., Hembree, G.G., et al., Standard Reference Materials: Development of a 1mm Diameter Particle Size Standard, SRM 1690, NBS Spec. Publ. 260-95 (May 1985). PB95-232518/AS**

Carpenter, B.S., Gramlich, J.W., Greenberg, R.R., et al., Standard Reference Materials: Uranium-235 Isotopic Abundance Standard Reference Materials for Gamma Spectrometry Measurements, NBS Spec. Publ. 260-96 (September 1986). PB87108544**

Mavrodineanu, R., and Gills, T.E., Standard Reference Materials: Summary of the Coal, Ore, Mineral, Rock, and Refactory Standards Issued by the National Bureau of Standards, NBS Spec. Publ. 260-97 (September 1985). PB86110830**

Hust, J.G., Standard Reference Materials: Glass Fiberboard SRM for Thermal Resistance, NBS Spec. Publ. 260-98 (August 1985). SN003-003-02674-3*

Callanan, J.E., Sullivan, S.A., and Vecchia, D.F., Standard Reference Materials: Feasibility Study for the Development of Standards Using Differential Scanning Calorimetry, NBS Spec. Publ. 260-99 (August 1985). PB86106747**

Taylor, J.K., Trahey, N.M., ed., Standard Reference Materials: Handbook for SRM Users, NBS Spec. Publ. 260-100 (February 1993). PB93183796**

Mangum, B.W., Standard Reference Materials: SRM 1970, Succinonitrile Triple-Point Standard: A Temperature Reference Standard Near 58.08° C, NBS Spec. Publ. 260-101 (March 1986). PB86197100**

Weidner, V.R., Mavrodineanu, R., Mielenz, K.D., et al., Standard Reference Materials: Holmium Oxide Solution Wavelength Standard from 240 to 640 nm - SRM 2034, NBS Spec. Publ. 260-102 (July 1986). PB86245727**

Hust, J.G., Standard Reference Materials: Glass Fiberblanket SRM for Thermal Resistance, NBS Spec. Publ. 260-103 (September 1985). PB86109949**

Mavrodineanu, R., and Alvarez, R., Standard Reference Materials: Summary of the Biological and Botanical Standards Issued by the National Bureau of Standards, NBS Spec. Publ. 260-104 (November 1985). PB86155561**

Mavrodineanu, R., and Rasberry, S.D., Standard Reference Materials: Summary of the Environmental Research, Analysis, and Control Standards Issued by the National Bureau of Standards, NBS Spec. Publ. 260-105 (March 1986). PB86204005**

Koch, W.F., ed., Standard Reference Materials: Methods and Procedures Used at the National Bureau of Standards to Prepare, Analyze, and Certify SRM 2694, Simulated Rainwater, and Recommendations for Use, NBS Spec. Publ. 260-106 (July 1986). PB86247483**

Hartman, A.W., and McKenzie, R.L., Standard Reference Materials: SRM 1965, Microsphere Slide (10 μm Polystyrene Spheres), NIST Spec. Publ. 260-107 (November 1988). PB89153704**

Mavrodineanu, R., and Gills, T.E., Standard Reference Materials: Summary of Gas Cylinder and Permeation Tube Standard Reference Materials Issued by the National Bureau of Standards, NBS Spec. Publ. 260-108 (May 1987). PB87209953**

Candela, G.A., Chandler-Horowitz, D., Novotny, D.B., et al., Standard Reference Materials: Preparation and Certification of an Ellipsometrically Derived Thickness and Refractive Index Standard of a Silicon Dioxide Film (SRM 2530), NIST Spec. Publ. 260-109 (October 1988). PB89133573**

Kirby, R.K., and Kanare, H.M., Standard Reference Materials: Portland Cement Chemical Composition Standards (Blending, Packaging, and Testing), NBS Spec. Publ. 260-110 (February 1988). PB88193347**

Gladney, E.S., O'Malley, B.T., Roelandts, I., et al., Standard Reference Materials: Compilation of Elemental Concentration Data for NBS Clinical, Biological, Geological, and Environmental Standard Reference Materials, NBS Spec. Publ. 260-111 (November 1987). PB88156708**

Marinenko, R.B., Blackburn, D.H., and Bodkin, J.B., Standard Reference Materials: Glasses for Microanalysis: SRMs 1871-1875, NIST Spec. Publ. 260-112 (February 1990). PB90215807**

Mangum, B.W., and Wise, J.A., Standard Reference Materials: Description and Use of a Precision Thermometer for the Clinical Laboratory, SRM 934, NIST Spec. Publ. 260-113 (June 1990). PB90257643**

Vezzetti, C.F., Varner, R.N., and Potzick, J.E., Standard Reference Materials: Bright-Chromium Linewidth Standard, SRM 476, for Calibration of Optical Microscope Linewidth Measuring Systems, NIST Spec. Publ. 260-114 (January 1991). PB91167163**

Williamson, M.P., Willman, N.E., and Grubb, D.S., Standard Reference Materials: Calibration of NIST SRM 3201 for 0.5 in. (12.65 mm) Serial Serpentine Magnetic Tape Cartridge, NIST Spec. Publ. 260-115 (February 1991). PB91187542**

Mavrodineanu, R., Burke, R.W., Baldwin, J.R., et al., Standard Reference Materials: Glass Filters as a Standard Reference Material for Spectrophotometry-Selection, Preparation, Certification and Use of SRM 930 and SRM 1930, NIST Spec. Publ. 260-116 (March 1994). PB94-188844/AS**

Vezzetti, C.F., Varner, R.N., and Potzick, J.E., Standard Reference Materials: Anti-reflecting-Chromium Linewidth Standard, SRM 475, for Calibration of Optical Microscope Linewidth Measuring Systems, NIST Spec. Publ. 260-117 (January 1992). PB92-149798**

Williamson, M.P., Standard Reference Materials: Calibration of NIST Standard Reference Material 3202 for 18-Track, Parallel, and 36-Track, Parallel Serpentine, 12.65 mm (0.5 in), 1491 cpmm (37871 cpi), Magnetic Tape Cartridge, NIST Spec. Publ. 260-118 (July 1992). PB92-226281**

Vezzetti, C.F., Varner, R.N., and Potzick, Standard Reference Materials: Antireflecting-Chromium Linewidth Standard, SRM 473, for Calibration of Optical Microscope Linewidth Measuring System, NIST Spec. Publ. 260-119 (September 1992)

Caskey, G.W., Philips, S.D., Borchardt., et al., Standard Reference Materials: A Users' Guide to NIST SRM 2084: CMM Probe Performance Standard, NIST Spec. Publ. 260-120 (1994)

Rennex, B.G., Standard Reference Materials: Certification of a Standard Reference Material for the Determination of Interstitial Oxygen Concentration in Semiconductor Silicon by Infrared Spectrophotometry, NIST Spec. Publ. 260-121 (1994) PB95-125076/AS

Gupta, D., Wang, L., Hanssen, L.M., Hsai, J.J., and Datla, R.U., Polystyrene Films for Calibrating the Wavelength Scale of Infrared Spectrophotometer (SRM 1921). NIST Spec. Publ. 260-122 (1995) PB95-226866/AS

Development of Technology and the Manufacture of Spectrometric SRMs for Naval Brasses (MC62 M63). NIST Spec. Publ. 260-123 (IN PREP)

Strouse, G.F., SRM 1744: Aluminum Freezing Point Standard. NIST Spec. Publ. 260-124 (1995) SN003-003-03342-1

Schiller, S.B, Standard Reference Materials: Statistical Aspects of the Certification of Chemical Batch SRMs. NIST Spec. Publ. 260-125 (1996) PB96-210877/AS

Guenther, F.R., Dorko, W.D., Miller, W.R., et al., Standard Reference Materials: The NIST Traceable Reference Material Program for Gas Standards, NIST Spec. Publ. 260-126 (1996) PB96-210786/AS

Strouse, G.F., ad Ahmet, A.T., Standard Reference Material 1747: Tin Freezing-Point Cell and Standard Reference Material 1748: Zinc Freezing-Point Cell, NIST Spec. Publ. 260-127 (IN PREP).

Zhang, Z.M., Gentile, T.R., Migdall, A.L., and Datla, R.U., "Transmission Filters with Measured Optical Density at 1064 nm Wavelength--Standard Reference Material 2036, NIST Spec. Publ. 260-128 (IN PREP).

Potzick, J.E., "Antireflecting-Chromium Linewidth Standard, Standard Reference Material 473, for Calibration of Optical Microscope Linewidth Measuring Systems", NIST Spec. Publ. 260-129 (IN PREP).

*Send order with remittance to: Superintendent of Documents, U.S. Government Printing Office, Washington, DC 20102. Remittance from foreign countries should include an additional one fourth of the purchase price for postage.

**May be ordered from: National Technical Information Services (NTIS), Springfield, VA 22161.
For information: (703-487-4650)
To Place an Order with PB#: (800-553-6847)

## TABLE OF CONTENTS

**PAGE**

## LIST OF TABLES

**PAGE**



## LIST OF FIGURES

## 1. Introduction

A Standard Reference Material (SRM) is a homogeneous and stable material which is measured accurately and certified as a reference material for purposes of evaluating a measurement process [1]. Thermal insulation SRMs provide certified values of thermal conductivity and resistance over a range of parameters, such as density and temperature. SRMs are intended primarily as a method for providing measurement assurance to user communities; for example, assistance in the calibration of heat-flow-meter apparatus and operation of guarded-hot-plate apparatus (ASTM Test Methods C 518 and C 177, respectively). The systematic use of common SRMs, including proper tracking with control charts, provides a means for accurate interlaboratory comparison of thermal conductivity data.

The development of SRMs in the United States has traditionally been one of the primary functions of the National Institute of Standards and Technology (NIST). In June 1995, the NIST Standard Reference Materials Program (SRMP) requested that the Building and Fire Research Laboratory initiate a research program to renew SRM 1450b, Fibrous Glass Board. The request for a renewal, now designated as SRM 1450c, was based on the relatively high demand for the SRM 1450 Series. Typically, sales of SRM 1450b averaged about 30 units annually. Like the previous lots of the SRM 1450 Series, the principal purpose for SRM 1450c was to assist industry in improving the acceptable accuracy of their processes for the measurement of thermal transmission properties of heat insulators under steady-state conditions.

Since the previous lot, SRM 1450b, had been characterized in the early and mid-1980's, SRMP requested an assessment of the current needs of industry by written questionnaire. Based on the responses, NIST procured a new lot of fibrous glass insulation boards from the same manufacturer of previous lots. Thermal conductivity measurements were conducted using the NIST one-meter line-heat-source guarded-hot-plate apparatus. Characterization of material properties was performed by the Building Materials Division and Polymers Division at NIST. This report describes the historical background of the SRM 1450 Series, assessment of industry's needs, material characterization, thermal conductivity measurements, regression analyses, certified values of thermal resistance, and uncertainty analyses of SRM 1450c.

## 2. Background

Historically, NIST has provided high-density fibrous glass insulation board as a reference material since 1958, purchasing separate lots of material designated by the year of acquisition. Thermal resistance measurements of the first four lots (1958, 1959, 1961, and 1970) were described by Siu [2]. In 1977, ASTM Committee C-16 on Thermal Insulation published a position paper [3] advocating the development of a Standard Reference Material (SRM) approach for proficiency in a proposed thermal accreditation program. In response, NIST established SRMs 1450 and 1450a using the remaining materials from the above internal lots. These first two SRMs were rapidly depleted due to limited stockpiles and two additional lots (1980 and 1981) were acquired for SRM 1450b. The thermal characterization of SRM 1450b was accomplished at NIST laboratory facilities in Gaithersburg, Maryland and Boulder, Colorado as described by Hust [4]. Table 1 summarizes the chronology of the SRM 1450 Series.

| Table 1<br>Chronology of the SRM 1450 Series, Fibrous Glass Board | | | | |
|---|---|---|---|---|
| **SRM** | **Issued** | **Thickness (mm)** | **Bulk Density ($kg/m^3$)** | **Temperature (K)** |
| SRM 1450 | 26 May 1978 | 25.4 | 100 to 180 | 255 to 330 |
| SRM 1450a | 12 Feb 1979 | 25.4 | 60 to 140 | 255 to 330 |
| SRM 1450b(I) | 21 May 1982 | 25.4 | 110 to 150 | 260 to 330 |
| SRM 1450b(II) | 20 May 1985 | 25.4 | 110 to 150 | 100 to 330 |
| SRM 1450c | new (1997) | 25.4 | 150 to 165 | 280 to 340 |

## 3. Questionnaire Results

In August 1995, a questionnaire requesting industry's input for SRM 1450c was mailed to 433 individuals assembled from the mailing rosters of ASTM Committee C-16 and the Standard Reference Material Program (SRMP). The recipients were asked to provide information on their measurement process including their measurement application, uncertainties, temperature range, specimen size, etc., and the requirements desired for SRM 1450c. Copies of the questionnaire and responding individuals and companies are provided in Appendix A. Forty-six (11 percent) of the questionnaires were returned before the deadline, which is fairly typical for similar mailings conducted by SRMP. The results were compiled and presented at the autumn meeting of the ASTM Committee C-16 Reference Materials Task Group in Providence, Rhode Island on October 3, 1995. A brief summary is provided below.

Sixteen of the 46 responses indicated that the recipient did not use SRM 1450, 1450a, or 1450b as part of their normal business activities. Those responses were subsequently discounted and only the statistical information from the remaining 30 questionnaires (hereafter identified as users) was included in the analysis. The majority of the 30 users were from either thermal insulation manufacturers or thermal testing companies, Figure 1a. The most common test methods were ASTM Test Methods C 518 and C 177, Figure 1b, and the most common test sizes were 305 mm and 610 mm square, Figure 1c. Interestingly, most of the users indicated that their measurement process was uncertain by less than 2 percent, Figure 1d. Several users indicated a wide range of thickness and temperature for their measurement process, Figures 2a and 2b, respectively.

Concerning the requirements for SRM 1450c, most users desired specimens having dimensions consistent with previous SRMs; that is, 610-mm square and 25.4-mm thick, Figures 3a and 3b, respectively. The desired temperature range was, for the most part, within the operating range of the NIST one-meter guarded-hot-plate apparatus, as illustrated in Figure 3c. The requests for extremely high temperatures were not possible, given an upper binder limit of approximately 200 °C for the material. Requests for extremely low temperatures (-150 °C) were, unfortunately, not possible with the current apparatus. Given the favorable approval of SRM 1450b, it was not unexpected that most users requested SRM 1450c be stockpiled within one to two years or sooner, Figure 4a. The majority of users also requested the same (nominal) bulk density, thermal conductivity, and manufacturer as for previous lots, Figures 4b and 4c.

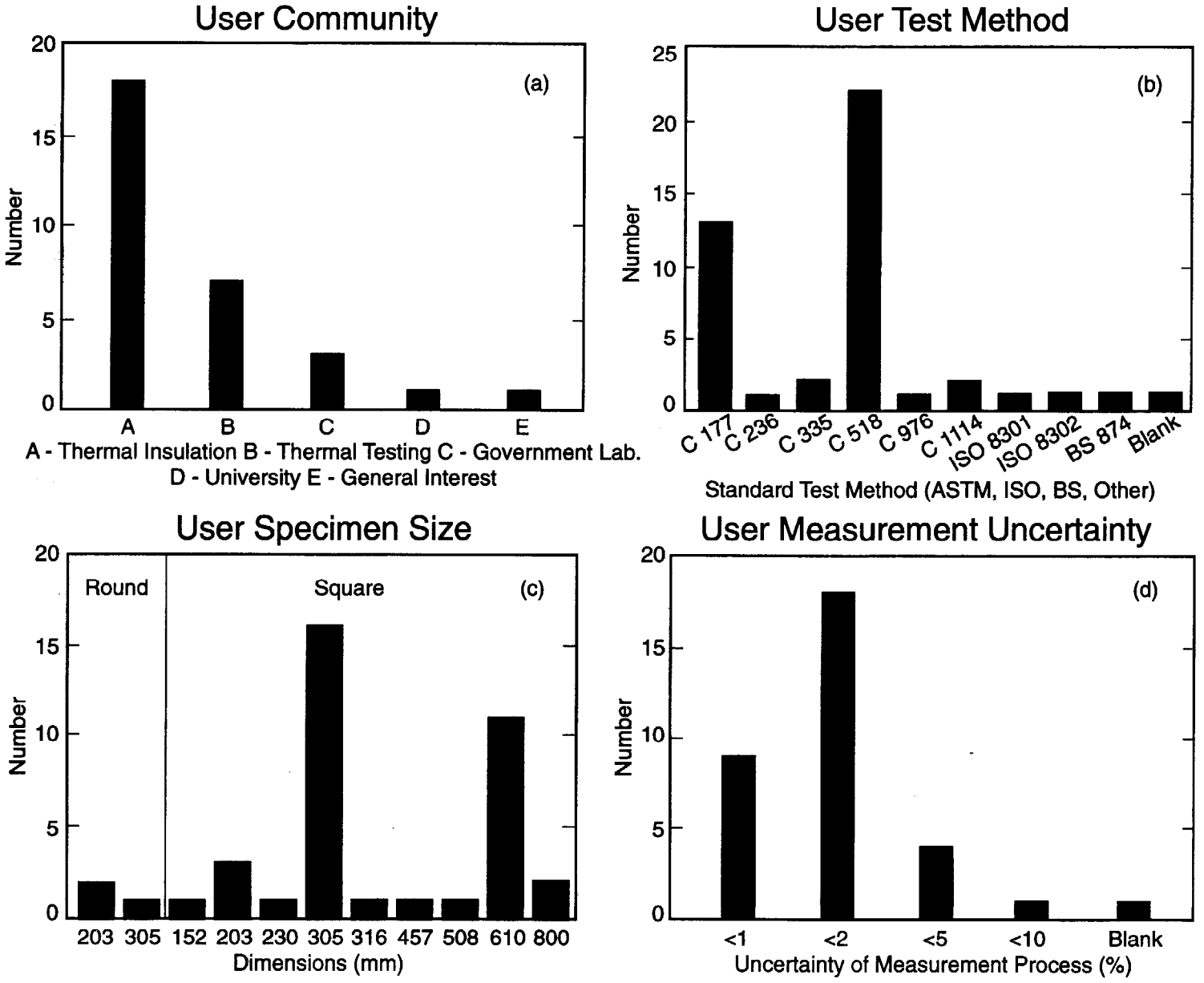


Figure 1. User Measurement Process

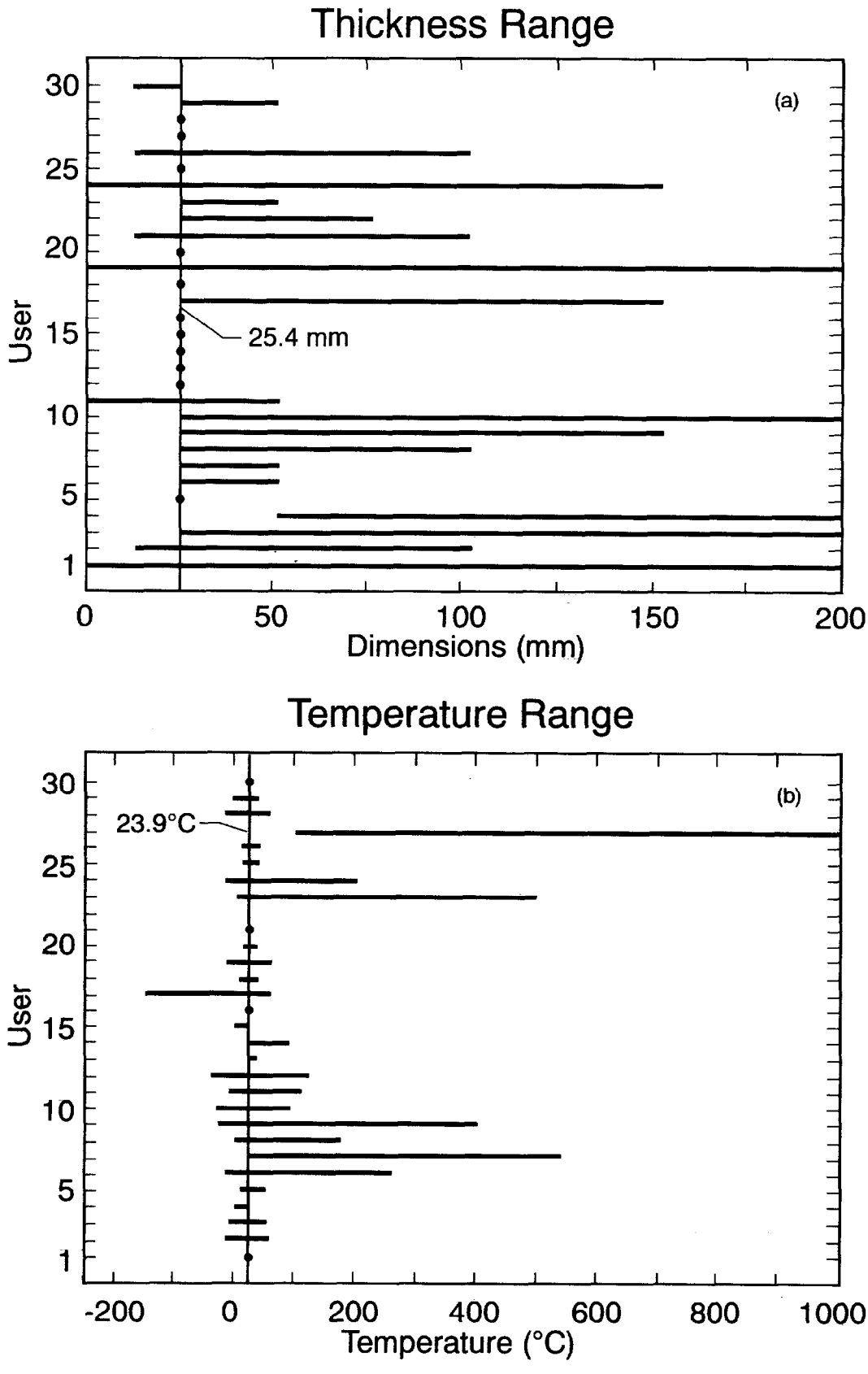


Figure 2. User Thickness and Temperature Ranges.

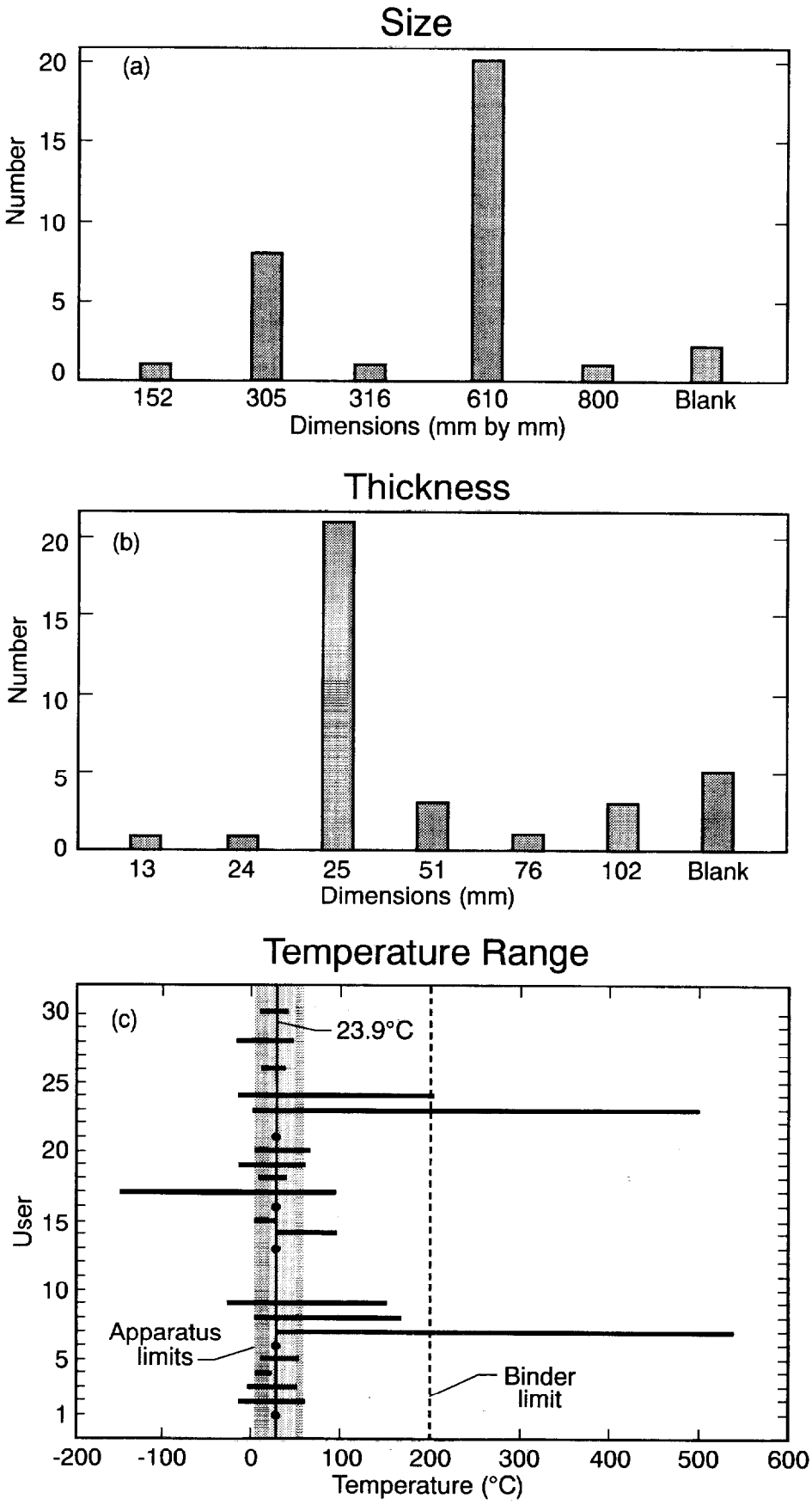


Figure 3. SRM technical requirements requested by users.

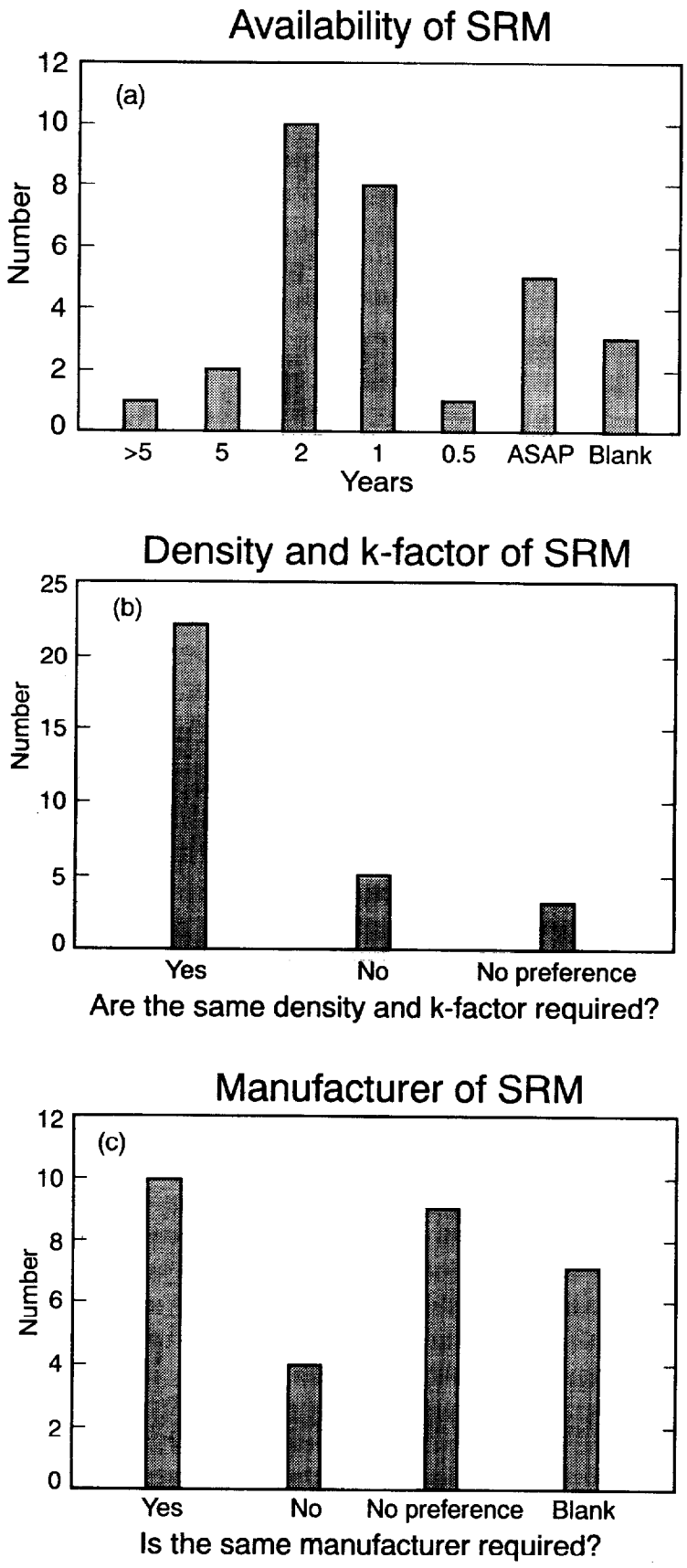


Figure 4. SRM logistical requirements requested by users.

## 4. Material Properties

This section describes the material properties of the fibrous glass thermal insulation, including the production of the material, statistical summary of the lot, inhomogeneities between and within board, thermogravimetry of the binder content, microstructure, compressive strength, and sorption isotherm. The sorption isotherm had been developed previously at NIST for similar commercial glass-fiber insulation.

### *Production of Material (Lot 1996)*

In May of 1996, NIST procured 130 boards of high-density fibrous glass thermal insulation from Owens Corning[1], designated internally as Lot 1996. The nominal dimensions of the boards, as purchased, were 1220 mm × 1220 mm × 25 mm thick, and the nominal density was 160 kg/m$^3$ (10 lb/ft$^3$). The material was manufactured by molding glass-fiber "pelts"and binder to produce a semi-rigid board. The fibers were oriented such that the lengths were essentially parallel to the board faces. The glass fibers were an alkali-alkaline alumino-borosilicate glass bound with a phenyl-formaldehyde binder, commonly referred to as "phenolic binder." After delivery, the boards were placed in a storage laboratory maintained at 21 EC to 26 EC and relative humidity that ranged from 45 percent to 60 percent.

### *Statistical Summary of Physical Properties*

In order to select the test specimens for this study, it was necessary to determine the mass, physical dimensions, and bulk density of each board. Measurements of all 130 boards were completed in 2 days. Table 2 gives summary statistics for the mass, length, width, thickness, and bulk density of the 130 boards. During this investigation, five boards were noted as either damaged (2) or anomalous (3) and were subsequently removed from the lot.

**Table 2**
**Summary Statistics for Fibrous Glass Boards, Lot 1996 (n = 130)**

| | Mass (g) | Length (mm) | Width (mm) | Thickness (mm) | Bulk Density (kg/m$^3$) |
|---|---|---|---|---|---|
| **Average** | 5895.4 | 1219.7 | 1219.7 | 25.36 | 156.34 |
| **Std. Dev.** | 91.5 | 0.5 | 0.5 | 0.05 | 3.64 |
| **Maximum** | 6058 | 1221 | 1221 | 29.0 | 162.7 |
| **Minimum** | 5085 | 1218 | 1218 | 24.5 | 136.3 |

### *Variations Among Boards*

[1] Certain commercial equipment, instruments, or materials are identified in this report to specify adequately the experimental procedure. Such identification does not imply recommendation or endorsement by NIST, nor does it imply that the materials or equipment are necessarily the best for the purpose.

Variations in the data for thickness and bulk density from board to board were analyzed graphically using a four-step method. The method consisted of (1) a run-sequence plot that checked for systematic and random changes; (2) a lag plot that checked for randomness; (3) a histogram that checked the frequency distribution; and, (4) a normal probability plot that checked for the normality assumption. These plots are useful in checking the underlying statistical assumptions in Table 2. Examples of the method are illustrated in Figures 5 and 6 for the board thickness and bulk density, respectively.

The thickness data in Figure 5 were taken at only a single point for this comparison. Two boards, 075 and 128, were found to contain a distended area resulting in a localized high thickness reading (Figure 5a). These boards were subsequently removed from the lot. The data in Figure 5 reveal that, with the exception of six boards of thickness greater than 26 mm, the thicknesses of the 130 boards are, in general, very consistent from board to board. The distribution of thicknesses is random, as shown by the tight cluster ("bull's-eye") of data points in the lag plot. Further, the distribution is normally distributed, as shown in the histogram and normality plot, about a mean value of 25.36 mm (see Table 2 for summary statistics). The relative standard deviation for the lot was 2.0 percent of the mean.

The bulk density data in Figure 6 were computed from single-point dimensional measurements and the mass of the board. The plots in Figure 6 revealed that board 013 had a very low bulk density due to an anomalously low mass. Consequently, board 013 was also removed from the lot. (Incidently, two other damaged boards, 045 and 130, were also removed.) The remainder of the data in Figure 6, however, appears quite consistent from board to board. The lag plot, excluding the low densities, reveals a random distribution of data points. The distribution of the data is normally distributed, as shown in the histogram and corresponding normality plot, about a mean of 156 kg/m$^3$ (9.8 lb/ft$^3$). The relative standard deviation for the lot was 2.3 percent.

### *Variations Within a Board*

The variation in density with respect to position within a board was examined by dividing board 130, (damaged during shipping) into 36 equal-size sections, each nominally 203 mm square. The bulk density of each 203 mm section was determined and the data were examined using the plots shown in Figure 7. The data, for the most part, are randomly distributed about a mean of 153.9 kg/m$^3$ (9.6 lb/ft$^3$) and the relative standard deviation for the board was 3.8 percent. This value is, unfortunately, somewhat higher than the relative standard deviation for the lot, indicating a greater variability within board than between boards. The variation of bulk density within board 130 is illustrated with the contour plot shown in Figure 8. The contour plot reveals variations across the board, ranging from 146 kg/m$^3$ to 164 kg/m$^3$. For these 203 mm square sub-samples, variations of this magnitude are not unexpected. Grimes [5] found similar variations in sub-samples of SRM 1450b. This within-board variation in density should not affect the (average) thermal conductivity of a board by more than 1 percent, as noted in Section 8. The source of the within-board variation in density was investigated below.

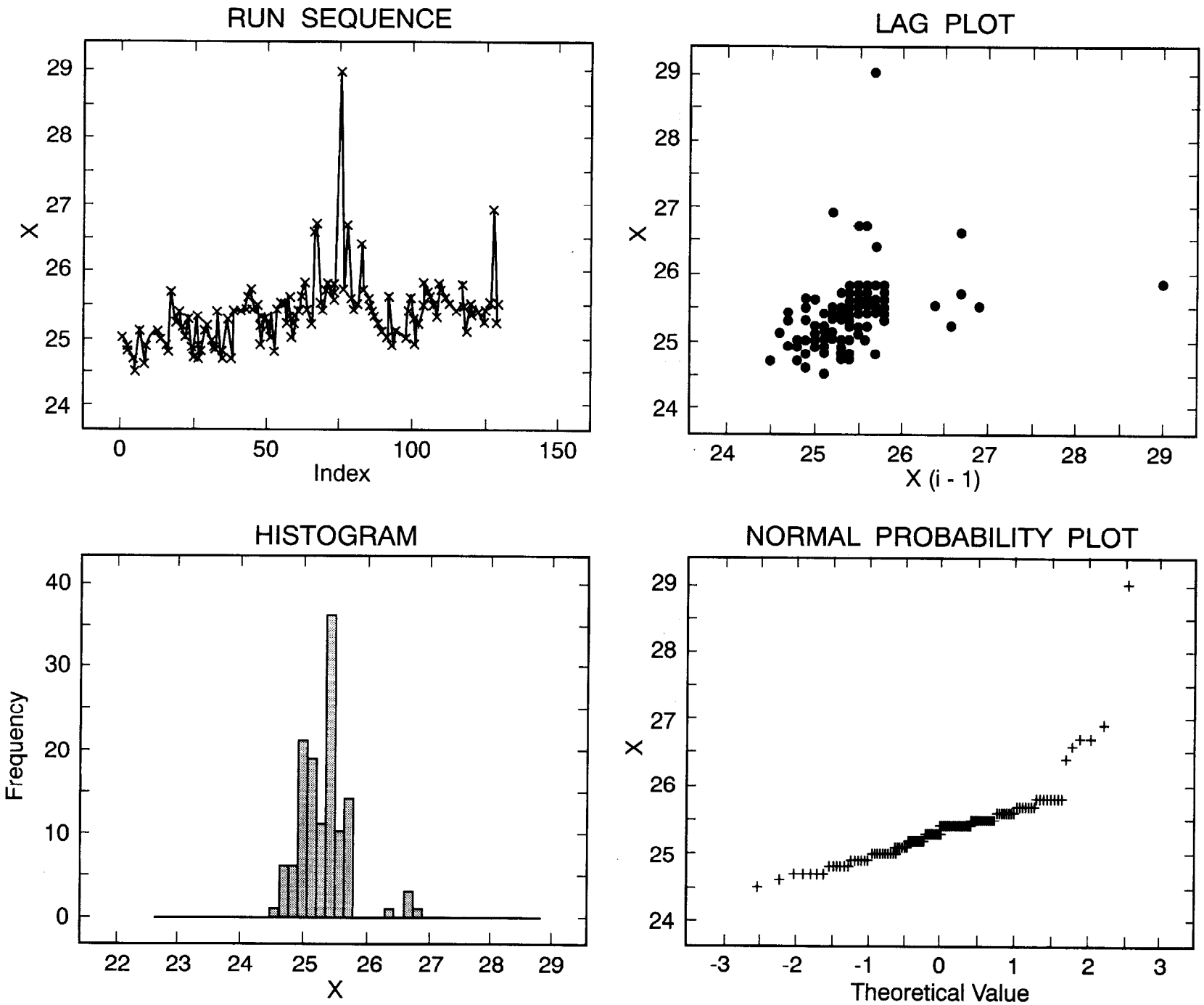


Figure 5. Global (between boards) variations of thickness; $\bar{L}$ = 25.36 mm, s ( $\bar{L}$ ) = 0.52 mm, n = 130.

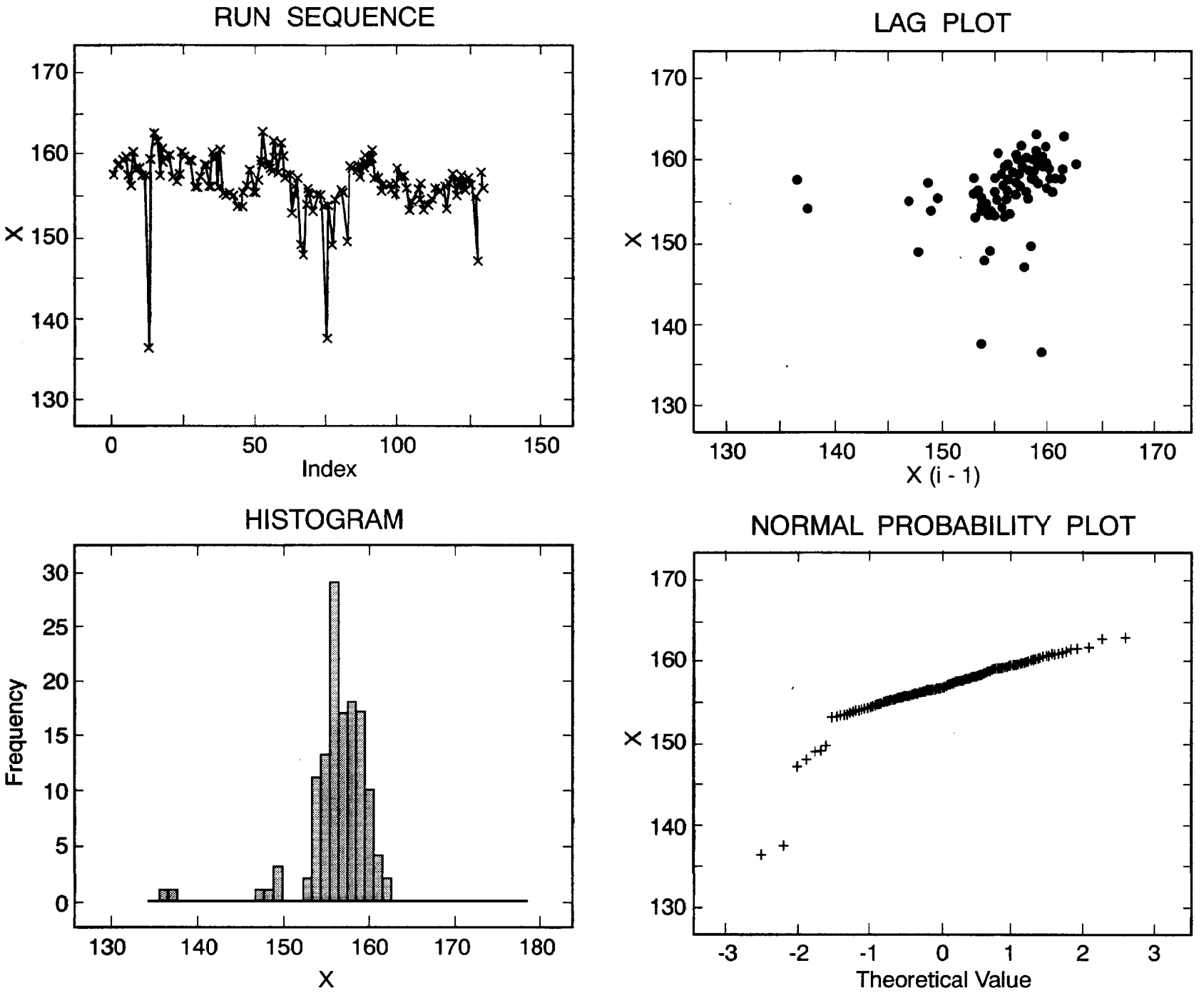


Figure 6. Global (between boards) variations of bulk density; $\bar{\rho}$ = 156.3 kg/m$^3$, s ($\bar{\rho}$) = 3.6 kg/m$^3$, n = 130.

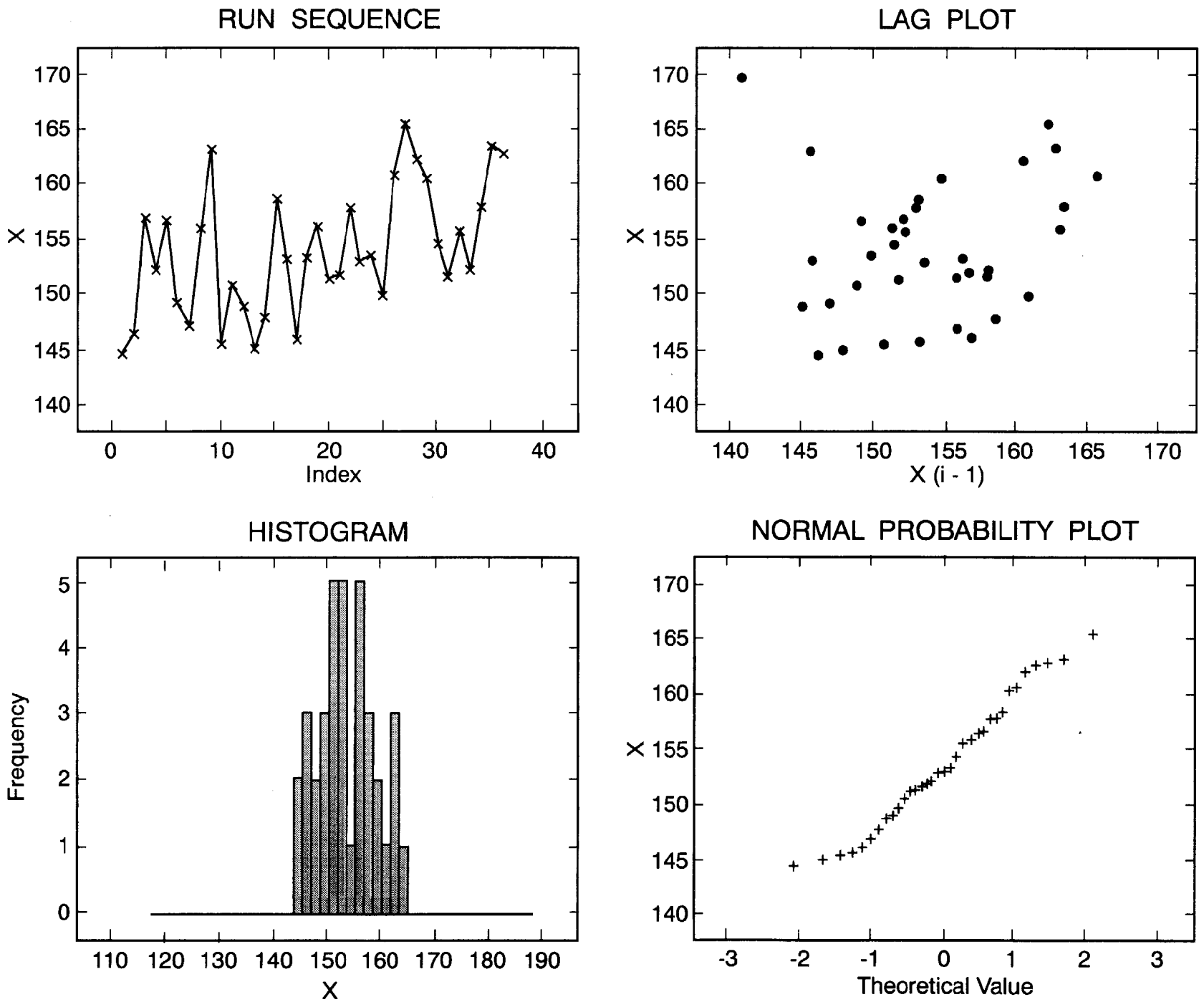


Figure 7. Local (within board) variations of bulk density for board 130; $\bar{\rho}$ = 153.9 kg/m$^3$, s ( $\bar{\rho}$ ) = 5.8 kg/m$^3$, ṅ = 36.

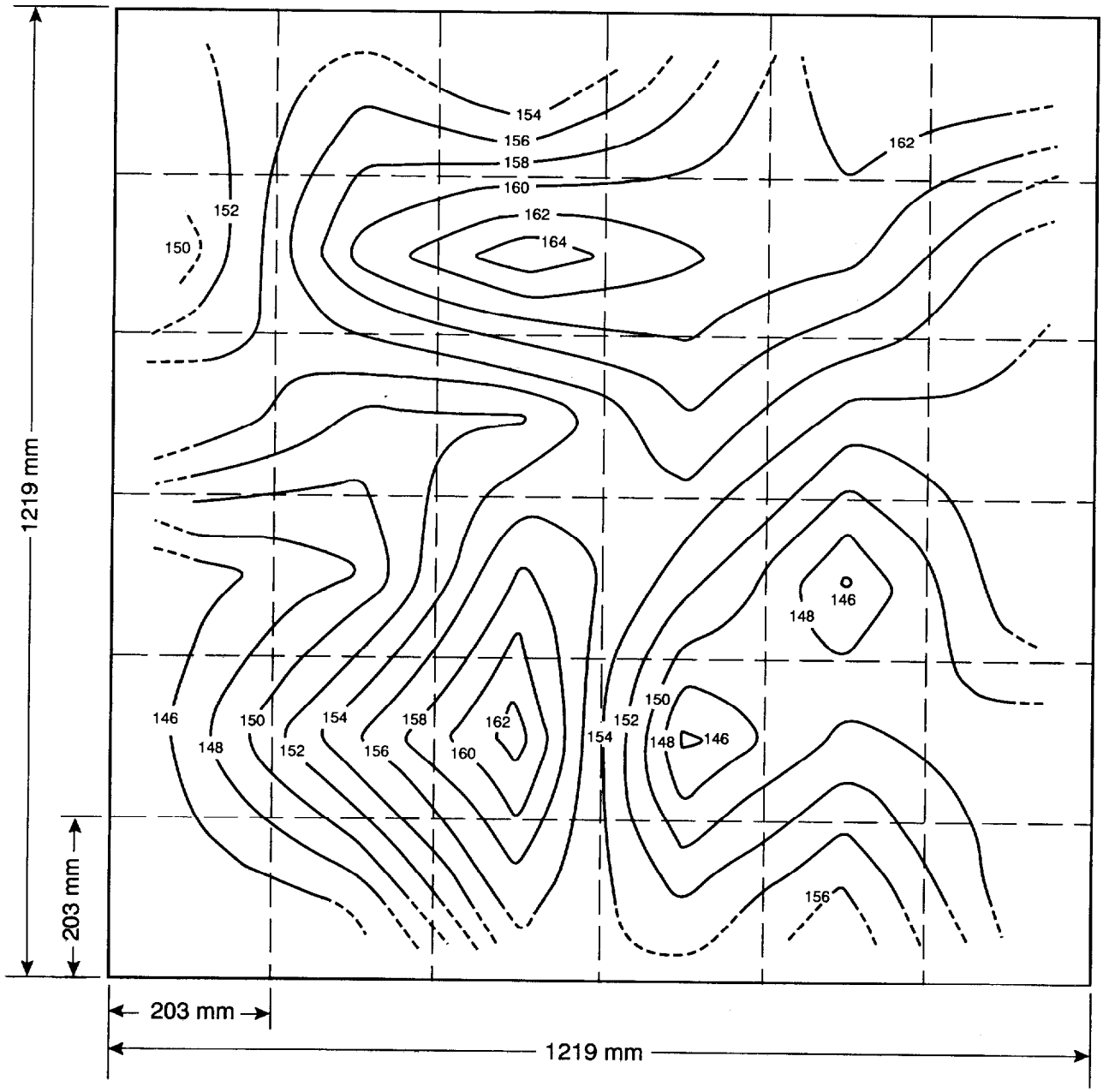


Figure 8. Contour plot of density variations (in kg/m$^3$) within board 130.

### *Binder Content Analysis*

The upper temperature limit of the phenolic binder was investigated by the NIST Polymers Division using thermogravimetry (TG). Six specimens, nominally 2 mm in diameter and 2 mm thick, were prepared from a sample of fibrous glass board, approximately 25 mm square. The masses of the specimens ranged from 3.169 mg to 7.052 mg. Each specimen was heated individually in an environment of air from room temperature to 800 °C at a rate of 10.0 °C per minute. The mass loss, in percent, of each specimen is plotted in Figure 9. The specimens gradually lost about 2 percent mass at 100 °C, presumably due to desorption of water vapor or other volatile compound(s). Above 200 °C, the mass loss was appreciable (Figure 9) and was most likely due to the chemical breakdown of the phenolic binder (and other organic compounds). For this reason, the upper temperature limit for the SRM was taken to be 200 °C (473 K). At 600 °C, all organic matter (i.e., binder) had been burned away, and only the glass fibers remained. The fractional mass loss (i.e., binder content) for the specimens ranged from 19.5 percent to 30.7 percent. This large variation was probably due, in part, to the small specimen size. In general, a larger specimen (e.g., 100 mm × 100 mm × 25 mm) is typically used to measure the binder content and the average binder content for this material would be expected to average between 15 percent and 20 percent by mass [6].

### *Microstructure*

The microcellular structure of the fibrous glass board was examined using a scanning electron microscope (SEM). Two small samples, showing the surface and cross-section views of the material, were cut from one board with a razor blade and sputter-coated with gold film, 20 nm thick, to prevent surface charging. Secondary electron images of the surface topography were obtained under operating conditions of 12 keV and a current of about 500 pA. Two images of the surface and cross-section views at a magnification of 75x are shown in Figures 10a and 10b, respectively. Note that in Figure 10a (surface view) the fibers are randomly oriented, and there is evidence of small globs of binder between some of the fibers. Figure 10b (cross-section) shows the stacked layers of glass fiber perpendicular to the direction of heat flow. The diameter of the fibers was estimated to be approximately 10 μm. The average fiber diameter expected for this material would be 6 μm to 8 μm on average as determined by air-flow resistance and micro-projection measurements [6].

### *Compressive Strength*

The compressive resistance was determined in accordance with ASTM Test Method C 165 [7], Procedure B, using a universal testing machine. Seven cylindrical specimens, nominally 100 mm in diameter by 25 mm thick, were cut from board 130 and conditioned at ambient laboratory conditions of 22 EC. The average bulk density of the seven specimens was 153.7 kg/m$^3$. The testing machine was operated at a cross head speed of 1 mm/min and data were collected at a rate of 50 points per second. Using the data from the load-deformation curve for each specimen, the compressive resistance was determined by:

$$S = \frac{W}{A}, \qquad \textbf{(1)}$$

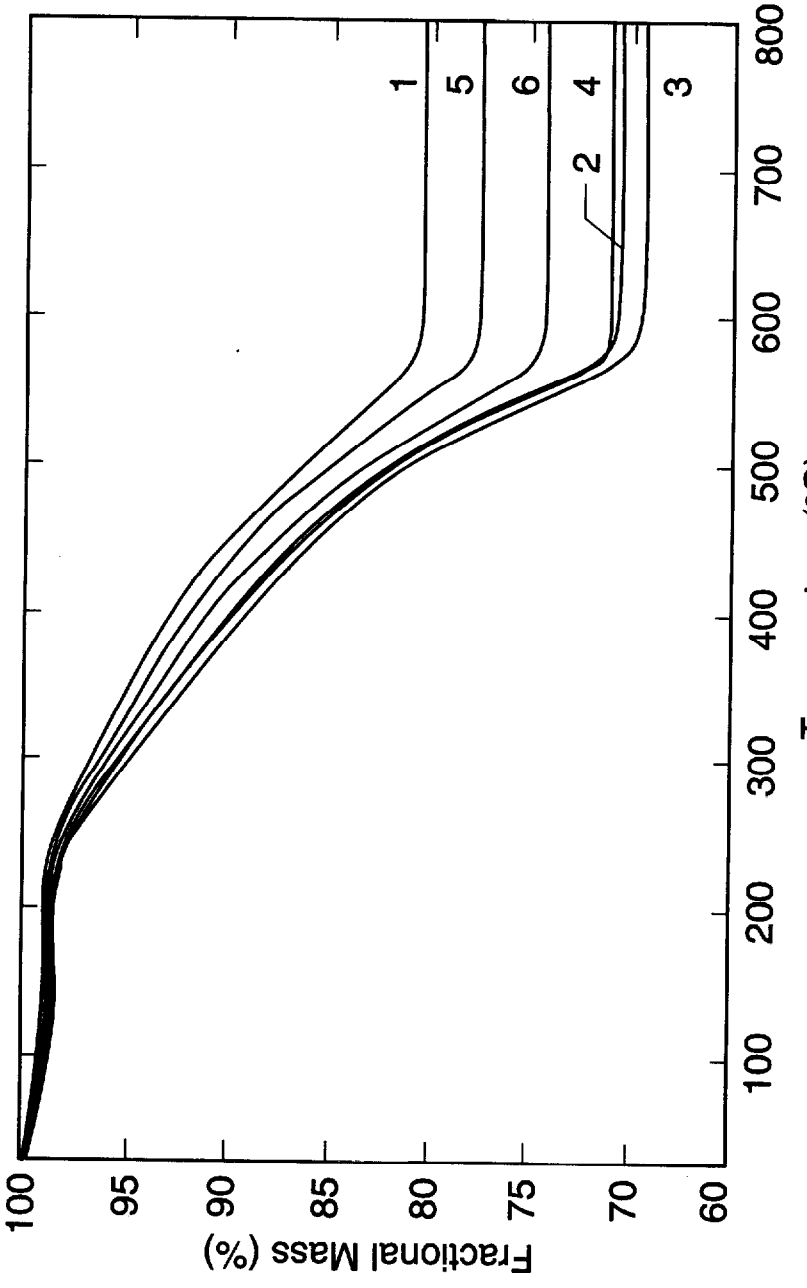


Figure 9. Thermogravimetry(TG) of phenolic binder content.

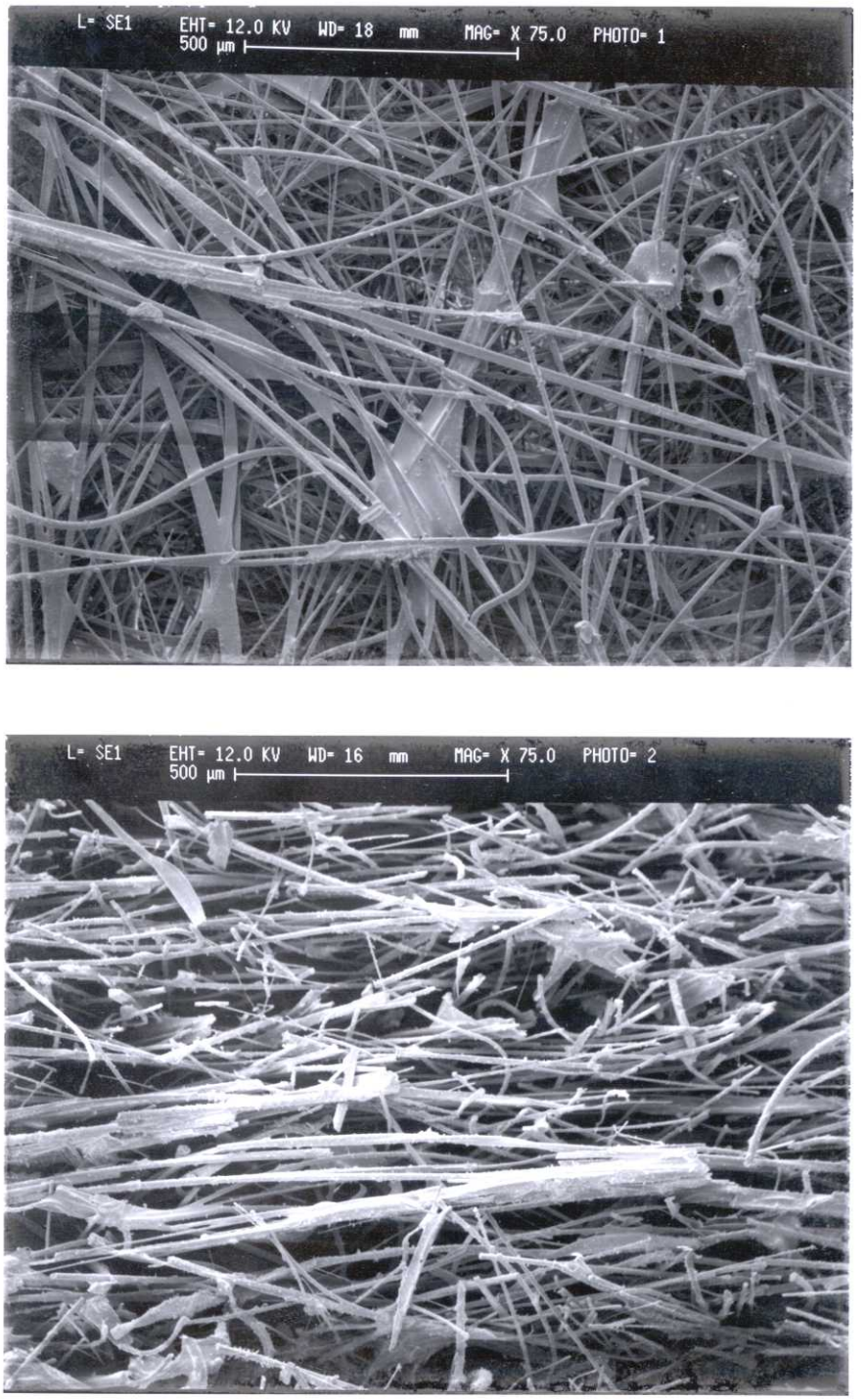


Figure 10. Microstructure of SRM 1450c, Fibrous Glass Board (a) surface view (b) cross-section view.

where

$W$ = compressive load at a given deformation and,
$A$ = original (undeformed) area, $m^2$.

The average compressive resistances for the specimens at deformations of 10 percent and 25 percent were 61 kPa and 157 kPa, respectively. The load-deformation curve departed from linearity at deformations above 28 percent. For thermal transmission testing, a small deformation of the specimen is required, typically on the order of 1 percent, in order to ensure proper thermal contact. Based on the compressive strength data, deformation of the SRM should not exceed 10 percent in order to prevent mechanical damage.

***Sorption Isotherm***

Sorption isotherms for a similar commercial glass-fiber insulation board had been determined by NIST in a previous set of experiments [8]. The moisture content of the glass-fiber insulation was determined using fixed-point humidities provided by aqueous salt solutions and desiccant drying, as opposed to oven drying. The masses of the specimens were determined at weekly time intervals until stable. Further details are available in Reference [8]. The sorption isotherm for the glass-fiber insulation is illustrated in Figure 11. The results are consistent with the analysis of the binder content. At typical laboratory conditions of 21°C and 50 percent relative humidity, the moisture content was less than 1 percent.

## 5. Specimens

The selection of test specimens was based on a full factorial experimental design (described later) that required three nominal levels of density. The intent was to reduce the possibility of the user having to extrapolate outside the range of values of bulk density provided in the Certificate for SRM 1450c. Based on the measurements of between-board density above, 30 boards were selected from Lot 1996 as follows: five pairs having the lowest density; five pairs about the median density; and, five pairs having the highest density. Using a sharp knife and metal template, one specimen, 1016 mm in diameter, was cut from the center of each board. ASTM Test Method C 177 [9] recommends that, whenever possible, the bulk density of the specimen be determined for the volume corresponding to the meter area of the test apparatus. In view of the within-board variability noted above, this recommendation was particularly appropriate. A 406-mm diameter cylinder, corresponding to the meter area of the apparatus, was cut from the center of each specimen and conditioned at nominal laboratory conditions of 24 °C and 50 percent relative humidity. The bulk densities for all 30 cylinders were determined, and the specimens were rank ordered by meter-area bulk densities, Table 3. The grand average and standard deviation were 159.6 $kg/m^3$ and 4.71 $kg/m^3$, respectively. The bulk densities ranged from 149.4 $kg/m^3$ to 167.3 $kg/m^3$, which was approximately the same range for Lot 1996 (Figure 6).

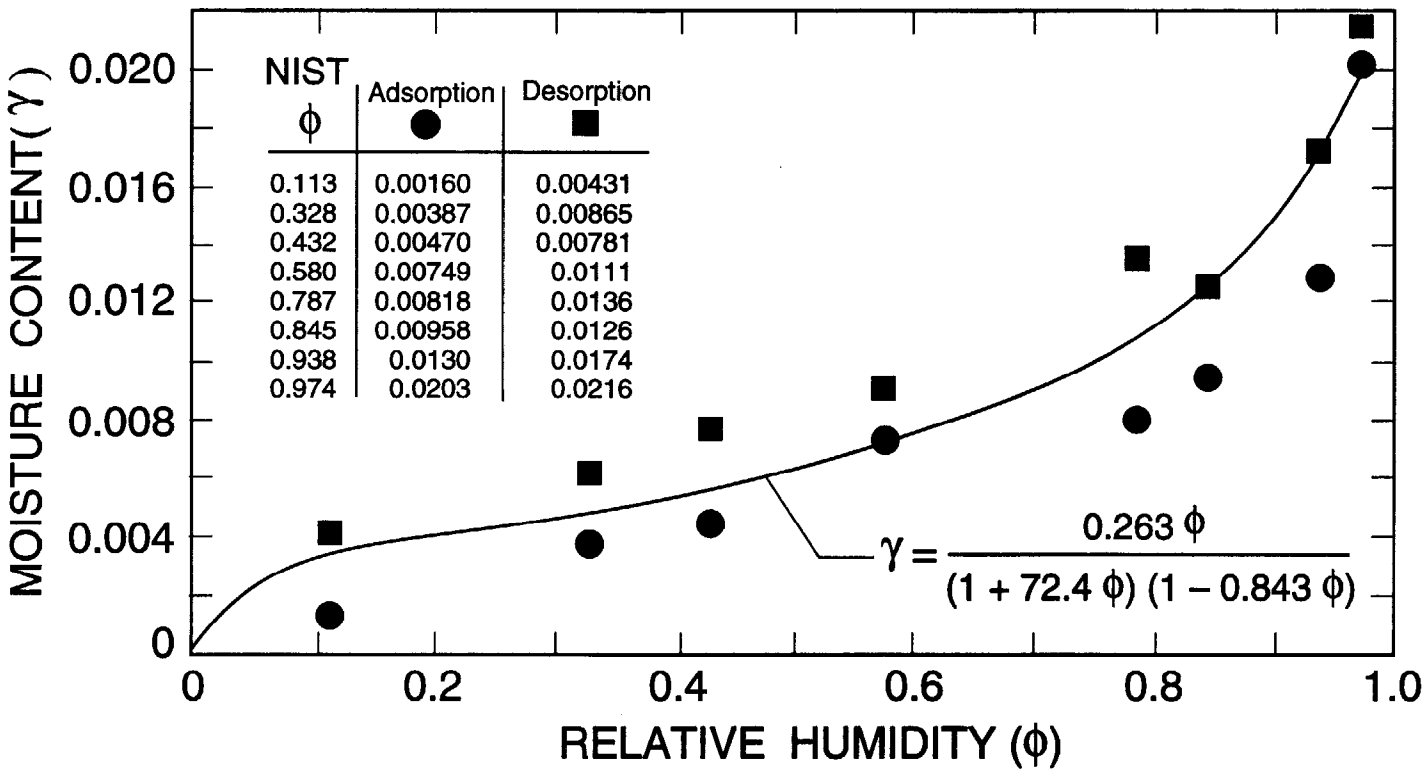


Figure 11. Sorption isotherm for a similar fibrous glass insulation (Source: Reference [8]).

| Table 3<br>Specimens Rank Ordered by Bulk Density of Meter Area (Laboratory Conditions) | | | | | | |
|---|---|---|---|---|---|---|
| **Pair** | **Nominal Density Level** | **ID 1** | **ID 2** | **Meter Area Bulk Density 1 ($kg/m^3$)** | **Meter Area Bulk Density 2 ($kg/m^3$)** | **Difference (%)** |
| 1 | Low | **77** | **97** | 151.2 | 149.4 | 1.2 |
| 2 | Low | **70** | **82** | 153.3 | 151.6 | 1.2 |
| 3 | Low | **67** | **93** | 155.8 | 156.2 | -0.2 |
| 4 | Low | **71** | **92** | 156.8 | 156.7 | 0.1 |
| 5 | Low | **104** | **109** | 157.5 | 156.8 | 0.4 |
| 6 | Mid | **35** | **101** | 157.9 | 157.6 | 0.2 |
| 7 | Mid | **66** | **108** | 158.3 | 158.1 | 0.1 |
| 8 | Mid | **51** | **118** | 159.3 | 159.5 | -0.1 |
| 9 | Mid | **7** | **53** | 160.5 | 159.9 | 0.4 |
| 10 | Mid | **38** | **63** | 161.3 | 161.0 | 0.2 |
| 11 | High | **91** | **117** | 163.4 | 162.1 | 0.8 |
| 12 | High | **23** | **59** | 163.5 | 163.8 | -0.2 |
| 13 | High | **18** | **25** | 164.6 | 163.9 | 0.4 |
| 14 | High | **16** | **57** | 165.9 | 166.5 | -0.4 |
| 15 | High | **15** | **124** | 167.3 | 166.8 | 0.3 |

## 6. Experimental

Measurements of thermal conductivity of the fibrous-glass specimens were determined in accordance with ASTM Test Method C 177 [9] using NIST's one-meter guarded-hot-plate apparatus. Each pair of specimens was measured once in a fully randomized sequence in order to minimize the introduction of bias in the test results. The measurements were generally completed in one to two days. This section describes the measurement procedure, uncertainties, and experimental design.

### *Measurements of Thermal Conductivity*

A schematic of the NIST one-meter line-heat-source guarded-hot-plate apparatus is shown in Figure 12. The apparatus has been described previously [10,11] and its operation is summarized briefly here. Two specimens having nearly the same density, size, and thickness are placed on the two sides of the guarded hot plate and clamped securely by the circular cold plates. Ideally, the guarded hot plate and cold plates provide constant-temperature boundary conditions to the surfaces of the specimens. With proper guarding in the lateral direction, the apparatus is designed to provide

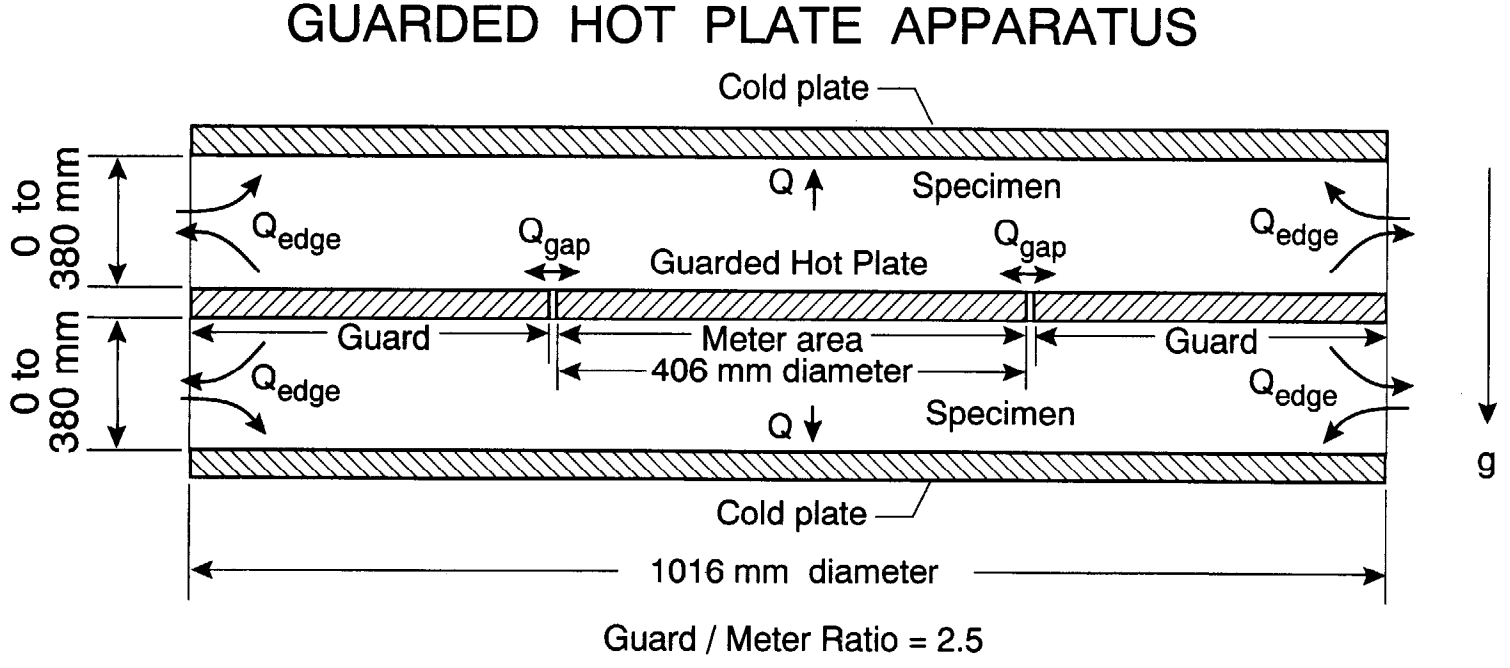


Figure 12. Schematic of NIST one-meter guarded hot plate. Heat flow: vertical.

one-dimensional heat flow ($Q$) through the meter area of the pair of specimens. Additional guarding was provided by a temperature-controlled environmental chamber that enclosed the test plates. In this case, the ambient temperature was maintained at the same value as the mean temperature ($T$) of the hot and cold plates.

During testing, data for $Q$ and the plate temperatures were collected every two minutes. Thermal equilibrium for the apparatus was attained when the plate temperatures were in a state of statistical control within 0.05 K of their target temperatures and $Q$ was also "in control." This means that values for the plate temperatures and $Q$ fluctuated randomly about a fixed level and the variation in fluctuations was also fixed. Steady-state data were collected for 4 h and averaged for the interval. Measurements of (apparent)[2] thermal conductivity ($\lambda$) for the pair of specimens were determined in accordance with ASTM Test Method C 177 [9] using the following equation:

$$Q = \lambda A \frac{\Delta T}{L}, \qquad \textbf{(2)}$$

where

$Q$ = heat flow through the meter area of the specimens, W;
$A$ = meter area normal to direction of heat flow, $m^2$;
$\Delta T = T_h - T_c$, temperature difference across specimens, K;
$T_h$ = hot plate temperature, K;
$T_c$ = cold plate temperature, K; and,
$L$ = thickness of specimens measured in situ, m.

Values of $\lambda$ were reported at the mean temperature ($T$) of the hot and cold plates, $T = \frac{1}{2}(T_h + T_c)$. In order to minimize the effect of moisture, the specimens were conditioned in an oven at 90 °C for a minimum of 16 h prior to testing. During testing, dry air was continuously injected into the environmental chamber decreasing the relative humidity to 15 percent or less, depending on the ambient dry bulb temperature ($T_a$). At the conclusion of each test, the specimen masses were measured. The maximum regain in mass was determined to be no more than 0.5 percent.

The effect of the meter-area incision was examined with a separate series of thermal conductivity tests. A pair of specimens was initially tested in the guarded-hot-plate apparatus before the meter area was cut. After cutting the meter area, the pair of specimens was retested in the guarded-hot-plate apparatus at the same conditions. The difference in the initial and final thermal conductivities was quite small, less than 0.05 percent, and was subsequently neglected.

[2] The thermal transmission properties of heat insulators determined from standard test methods typically include several mechanisms of heat transfer, including conduction, radiation, and possibly convection. For that reason, some experimentalists will include the adjective "apparent" when describing thermal conductivity of thermal insulation. However, for brevity, the term thermal conductivity will be used in this report.

***Measurements of Bulk Density***

The bulk densities (ρ) of the 406-mm-diameter meter area were determined in accordance with ASTM Test Method C 177 [9] by dividing the mass ($m$) of the cylinder by its corresponding volume ($V$), or:

$$\rho = \frac{m}{V}. \quad \textbf{(3)}$$

The mass was obtained by using a precision balance having a sensitivity of 0.1 g. The diameters of the cylinders were measured at two locations using a steel rule having a resolution of 0.5 mm. The thickness for the 406-mm diameter was averaged from five measurements taken on a granite flat table with a precision caliper, 0.1 mm resolution.

***Uncertainty in Measurements***

The measurement uncertainties for thermal conductivity, mean temperature, and bulk density were derived in accordance with current ISO guidelines [12,13] and are described in Appendices B and C, respectively. The standard uncertainties for the thermal conductivity, mean temperature, and bulk density were 0.00020 W/(m⋅K), 0.034 K, and 0.72 kg/m$^3$, respectively. These standard uncertainties were included in the combined standard uncertainty for predicted values of thermal conductivity, $u_c(\hat{\lambda})$, as described in Section 9.

***Design***

Based on previous experience [2,4], a model for thermal conductivity (λ) as a function of bulk density (ρ) and mean temperature ($T$) was assumed to be

$$\lambda(\rho,T) = a_0 + a_1\rho + a_2T + a_3T^2 + a_4T^3. \quad \textbf{(4)}$$

In order to check the adequacy of eq (4), a full factorial design with 3 levels for ρ and 5 levels for $T$ was selected, Table 4. This design also allowed checking for the necessity of: a quadratic term for ρ, a fourth-order term for $T$, and/or a cross-product term for ρ and $T$ in order to model the data.

**Table 4**
**Full Factorial (3 by 5) Experimental Design-Replicates, (Sequence)**

| Density Level | Temperature Level (K) | | | | |
|---|---|---|---|---|---|
| | **280** | **295** | **310** | **325** | **340** |
| High | 1, (15) | 1, (04) | 1, (05) | 1, (14) | 1,(10) |
| Mid | 1, (07) | 1, (13) | 1, (09) | 1, (01) | 1, (12) |
| Low | 1, (06) | 1, (11) | 1, (02) | 1, (08) | 1, (03) |

**7. Results**

### *Meter-Area Bulk Density*

The 15 pairs of specimens were tested in the guarded-hot-plate apparatus following the test sequence given in Table 5, which randomized both independent variables, $T$ and ρ. The top and bottom specimens were identified with subscripts 1 and 2, respectively. The meter-area bulk density was determined at the conclusion of each test and the average meter-area bulk density was computed for each pair of specimens. The average moisture regain for the 30 specimens was 0.4 percent (12 g). The average meter-area bulk densities ranged from 149.4 kg/m$^3$ to 166.0 kg/m$^3$.

**Table 5**
**Final Meter Area Bulk Densities for SRM 1450c Specimens**

| Test Sequence | Test Number | T (K) | Nominal ρ | $ID_1$ | $\rho_1$ (kg/m$^3$) | $ID_2$ | $\rho_2$ (kg/m$^3$) | Average ρ |
|---|---|---|---|---|---|---|---|---|
| 1 | 96-008A | 325 | M | **7** | 159.5 | **53** | 158.9 | 159.2 |
| 2 | 96-009A | 310 | L | **70** | 152.3 | **82** | 150.7 | 151.5 |
| 3 | 96-010A | 340 | L | **67** | 154.7 | **93** | 155.0 | 154.8 |
| 4 | 96-011A | 295 | H | **18** | 163.5 | **25** | 163.0 | 163.2 |
| 5 | 96-012A | 310 | H | **23** | 162.3 | **59** | 162.8 | 162.6 |
| 6 | 96-013A | 280 | L | **71** | 155.9 | **92** | 155.7 | 155.8 |
| 7 | 96-014A | 280 | M | **51** | 158.4 | **118** | 158.5 | 158.5 |
| 8 | 96-015A | 325 | L | **77** | 150.4 | **97** | 148.4 | 149.4 |
| 9 | 96-016A | 310 | M | **38** | 160.2 | **63** | 160.0 | 160.1 |
| 10 | 96-017A | 340 | H | **16** | 164.6 | **57** | 165.2 | 164.9 |
| 11 | 96-018A | 295 | L | **104** | 156.4 | **109** | 155.7 | 156.1 |
| 12 | 96-019A | 340 | M | **35** | 156.7 | **101** | 156.3 | 156.5 |
| 13 | 96-020A | 295 | M | **66** | 157.2 | **108** | 157.1 | 157.1 |
| 14 | 96-021A | 325 | H | **91** | 162.2 | **117** | 160.7 | 161.5 |
| 15 | 96-022A | 280 | H | **15** | 166.3 | **124** | 165.7 | 166.0 |

### *Thermal Conductivity*

Table 6 summarizes the experimental test conditions and measured thermal conductivity (λ) for each pair of specimens. Note that an extra digit is provided for λ to reduce rounding errors. Each test was conducted with heat flow in the vertical direction and a temperature difference of 20 K across the specimens. During a test, the ambient temperature ($T_a$) of the air surrounding the specimens was maintained at the same value of the mean temperature ($T$) by means of a temperature-controlled environmental chamber. The ambient air pressure ($P_a$) was not controlled, but varied with barometric conditions. The relative humidity (RH) varied with the chamber's dry-bulb temperature.

Several parameters in Table 6 indicate the "average" value for the top and bottom specimen, i.e., bulk

density (ρ), thickness (*L*), clamping load, etc. The average thickness (*L*) was determined from in-situ measurements of the top and bottom plate separation. The grand average of the test thicknesses was 25.33 ± 0.22 mm (one standard deviation, 1s). The grand average of the clamping loads was 475 ± 217 N (1s) which varied from test to test (Table 6) due to the thermal expansion and contraction of the specimens and the apparatus. The maximum clamping pressure of 1 kPa (Table 6) was well below the compression limit established in Section 4.

**Table 6**
**Thermal Conductivity Measurements of SRM 1450c**

| Test | T (K) | $\rho_{avg}$ (kg/m$^3$) | $L_{avg}$ (mm) | Load* (N) | $T_a$ (K) | $P_a$ (kPa) | RH (%) | $T_h$ (K) | $T_{c,avg}$ (K) | λ (W/(m·K)) |
|---|---|---|---|---|---|---|---|---|---|---|
| 1 | 325 | 159.2 | 25.07 | 648 | 325.2 | 100.48 | <5 | 335.15 | 315.15 | 0.03679 |
| 2 | 310 | 151.5 | 25.88 | 458 | 310.2 | 100.90 | <5 | 320.15 | 300.15 | 0.03439 |
| 3 | 340 | 154.8 | 25.39 | 850 | 340.2 | 100.63 | <5 | 350.15 | 330.15 | 0.03777 |
| 4 | 295 | 163.2 | 25.15 | 359 | 295.2 | 101.34 | <10 | 305.15 | 285.15 | 0.03340 |
| 5 | 310 | 162.6 | 25.27 | 321 | 310.2 | 101.14 | <10 | 320.15 | 300.15 | 0.03499 |
| 6 | 280 | 155.8 | 25.51 | 72 | 280.2 | 100.40 | 15 | 290.15 | 270.15 | 0.03143 |
| 7 | 280 | 158.5 | 25.16 | 430 | 280.1 | 100.46 | 14 | 290.15 | 270.15 | 0.03166 |
| 8 | 325 | 149.4 | 25.09 | 626 | 325.2 | 100.10 | <5 | 335.15 | 315.16 | 0.03597 |
| 9 | 310 | 160.1 | 25.29 | 479 | 310.2 | 101.60 | <5 | 320.15 | 300.15 | 0.03534 |
| 10 | 340 | 164.9 | 25.35 | 770 | 340.2 | 101.24 | <5 | 350.15 | 330.15 | 0.03828 |
| 11 | 295 | 156.1 | 25.42 | 200 | 295.2 | 100.87 | <10 | 305.15 | 285.15 | 0.03297 |
| 12 | 340 | 156.5 | 25.01 | 701 | 340.2 | 100.69 | <5 | 350.15 | 330.15 | 0.03798 |
| 13 | 295 | 157.1 | 25.39 | 308 | 295.2 | 100.67 | <10 | 305.15 | 285.14 | 0.03272 |
| 14 | 325 | 161.5 | 25.42 | 543 | 325.2 | 101.03 | <5 | 335.15 | 315.16 | 0.03648 |
| 15 | 280 | 166.0 | 25.55 | 352 | 280.2 | 100.39 | 14 | 290.15 | 270.15 | 0.03199 |

*Plate Surface Area = 0.811 m$^2$.

## 8. Analysis

### *Multiple Variable Regression Analysis*

The thermal conductivity (λ) as a function of specimen bulk density (ρ) and mean temperature (*T*) is shown in Figures 13a and 13b, respectively. Both plots show a positive correlation for λ and the independent variables. That is, λ increased (linearly) with increasing levels of ρ or *T*, although the change with respect to ρ was small (Figure 13a) in comparison to the effect of *T* (Figure 13b). There were, however, small inconsistencies in the data. As noted in Figure 13a, the change in λ was not monotonic for some temperature levels. For example, at 325 K the value of λ for the highest density specimen was lower than the value of λ for the mid-density specimen. These inconsistencies were

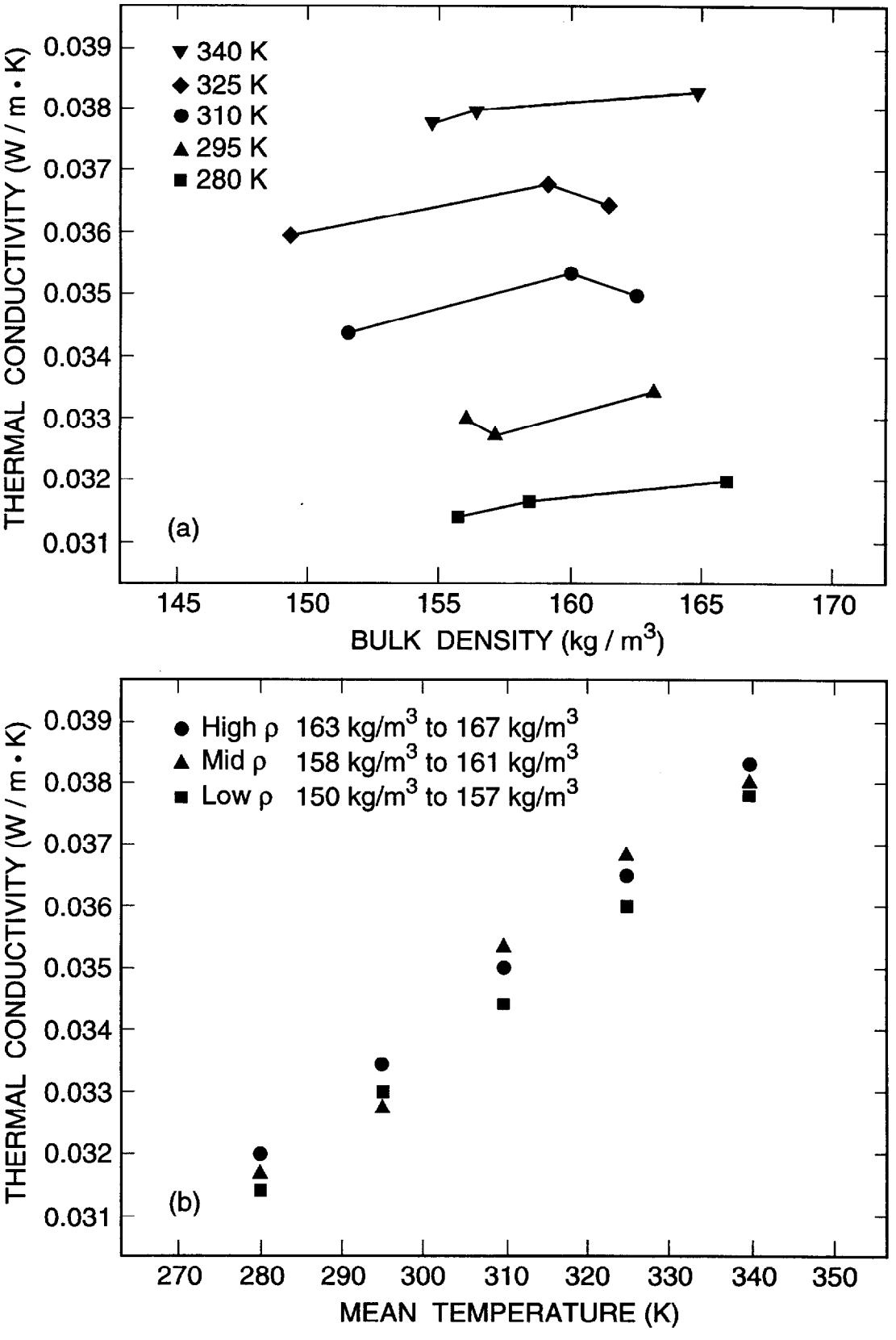


Figure 13. (a) Thermal conductivity as a function of bulk density.
(b) Thermal conductivity as a function of mean temperature.

also present in Figure 13b where, for a given temperature, the data points were not necessarily arranged from the lowest to highest density. The cause of the variabilities was unknown but most likely was due to between-specimen variability such as localized density variations, noted above.

The data for the bulk density, mean temperature, and corresponding value of thermal conductivity were fit to the $\lambda(\rho,T)$ model, eq (4), by a multiple variable regression analysis. Higher order temperature terms were determined to be statistically insignificant, and so a final form, linear in $\rho$ and $T$, was acceptable. The final model is

$$\hat{\lambda} = -7.7663\times10^{-3} + 5.6153\times10^{-5}\rho + 1.0859\times10^{-4}T. \quad \textbf{(5)}$$

The last digit of each coefficient is provided to reduce rounding errors. It is interesting to note that the prediction models for all previous lots of the SRM 1450 Series included a nonlinear term for temperature [2,4]. These previous lots (Table 1) were characterized using different guarded-hot-plate apparatus, a larger temperature range, particularly for SRM 1450b, and different experimental designs from that of the current study. In this study, higher-order temperature terms in the model did not improve the results of the curve fit. The author acknowledges that, for a larger temperature range, the above model is probably unacceptable. For this reason, the author strongly advises against extrapolation of the model beyond the temperature range of this study, 280 K to 340 K.

The residual standard deviation for the above fit was 0.000205 W/(m·K) which is quite small. The adequacy of the fit was further examined by plotting the individual deviations ($\delta$) from the model as defined by

$$\delta = \lambda - \hat{\lambda}. \quad \textbf{(6)}$$

Individual deviations versus $\rho$ and $T$ are shown in Figures 14a and 14b, respectively. The data in Figures 14a and 14b do not indicate any trends in the deviations, signifying a satisfactory fit. The majority of the deviations were within ± 0.00025 W/(m·K) of the measured values. The relative standard deviation multiplied by 2 for the fitted model was 1.1 percent. For comparison, the relative standard deviation multiplied by 2 for the fitted model of SRM 1450b was 1.5 percent [4].

The standard uncertainties ($u(\hat{\lambda})$) for predicted values of thermal conductivity were derived in accordance with international guidelines [12,13]. In general, values of $u(\hat{\lambda})$ increased near the extreme values (upper and lower) of $\rho$ and $T$. That is, the further away from the median values of $\rho$ and $T$, the lower the precision of the model. A maximum value of 0.00014 W/(m·K) at 150 kg/m$^3$ and 280 K was selected as a conservative estimate for the standard uncertainty of $\hat{\lambda}$.

### *Comparison to Interlaboratory Results and the SRM 1450 Series*

Recently, NIST has submitted for publication [14] the results of an international round robin conducted under the auspices of the International Organization for Standardization (ISO) Technical Committee TC 163 (Thermal Insulation). Test specimens were cut from a similar lot of fibrous glass board having a nominal bulk density of 164 kg/m$^3$ and subsequently circulated to laboratories in

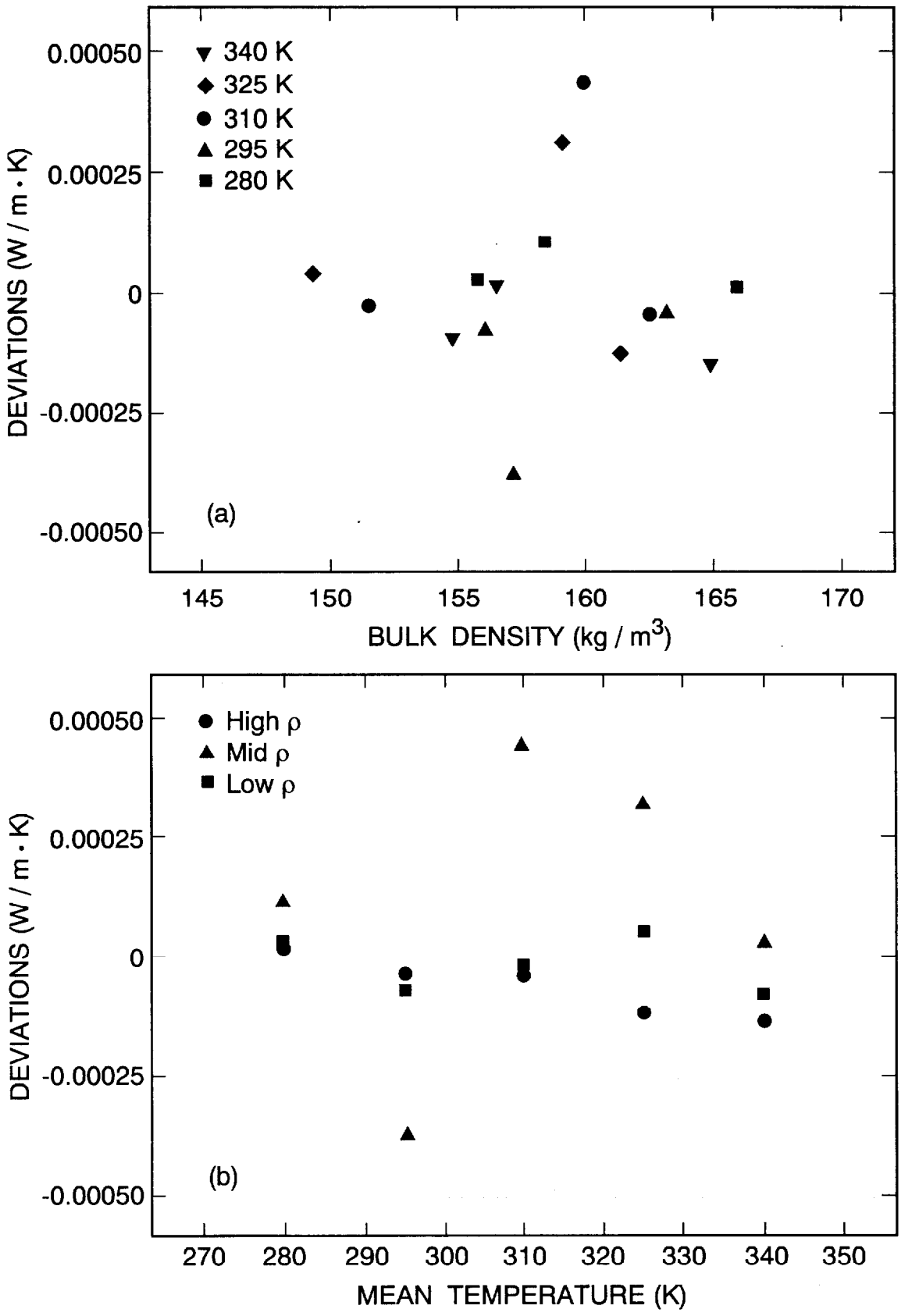


Figure 14. Scatter plots. (a) Deviations versus bulk density.
(b) Deviations versus mean temperature.

Europe, North America, Asia, and Australia. The participating laboratories were requested to measure the thermal conductivity at three mean temperatures of approximately 283 K, 297 K, and 313 K, using either guarded-hot-plate apparatus or heat-flow-meter apparatus.

The thermal conductivity data for the ISO Round Robin for North America and SRM 1450c are plotted in Figure 15 as a function of bulk density and mean temperature. The round robin data from NIST, which were determined in 1984 with the same apparatus used in this study (but with a different operator), are shown as triangles. The agreement among the sets of data is quite good, although the data for SRM 1450c appear to be somewhat lower than previous NIST data at temperatures of 280 K and 295 K (Figure 15b).

Using the regression models obtained for the ISO Round Robin [14] and the SRM 1450 Series, the predicted thermal conductivities of these lots were compared over the temperature range of 255 K to 340 K. The bulk density was fixed at 160 kg/m$^3$, which was the approximate average of SRM 1450c (Table 2). Unfortunately, the selection of this value for density required extrapolating for the models for SRMs 1450a and 1450b (Table 1). The most general model for these lots of materials was taken from Hust [4]:

$$\lambda(\rho,T) = b_0 + b_1\rho + b_2 T + b_3 T^3 + b_4 \exp\left[-\left(\frac{T-180}{75}\right)\right]^2. \qquad \textbf{(7)}$$

The regression coefficients for the models for the ISO Round Robin and the SRM 1450 Series are summarized in Table 7.

**Table 7**
**Regression Coefficients for the ISO Round Robin [14] and SRM 1450 Series**

| ISO R.R. & SRM | $b_0$ | $b_1$ | $b_2$ | $b_3$ | $b_4$ |
|---|---|---|---|---|---|
| ISO Round Robin | $9.578\times10^{-3}$ | $2.650\times10^{-5}$ | $4.570\times10^{-5}$ | $2.552\times10^{-10}$ | 0 |
| SRM 1450 | $1.7062\times10^{-2}$ | $3.648\times10^{-5}$ | 0 | $4.037\times10^{-10}$ | 0 |
| SRM 1450a | $1.930\times10^{-2}$ | $1.534\times10^{-5}$ | 0 | $4.256\times10^{-10}$ | 0 |
| SRM 1450b(I) | $1.645\times10^{-3}$ | $2.2122\times10^{-5}$ | $9.2087\times10^{-5}$ | $1.0753\times10^{-10}$ | 0 |
| SRM 1450b(II) | $-2.228\times10^{-3}$ | $2.743\times10^{-5}$ | $1.063\times10^{-4}$ | $6.473\times10^{-11}$ | $1.157\times10^{-3}$ |
| SRM 1450c | $-7.7663\times10^{-3}$ | $5.6153\times10^{-5}$ | $1.0859\times10^{-4}$ | 0 | 0 |

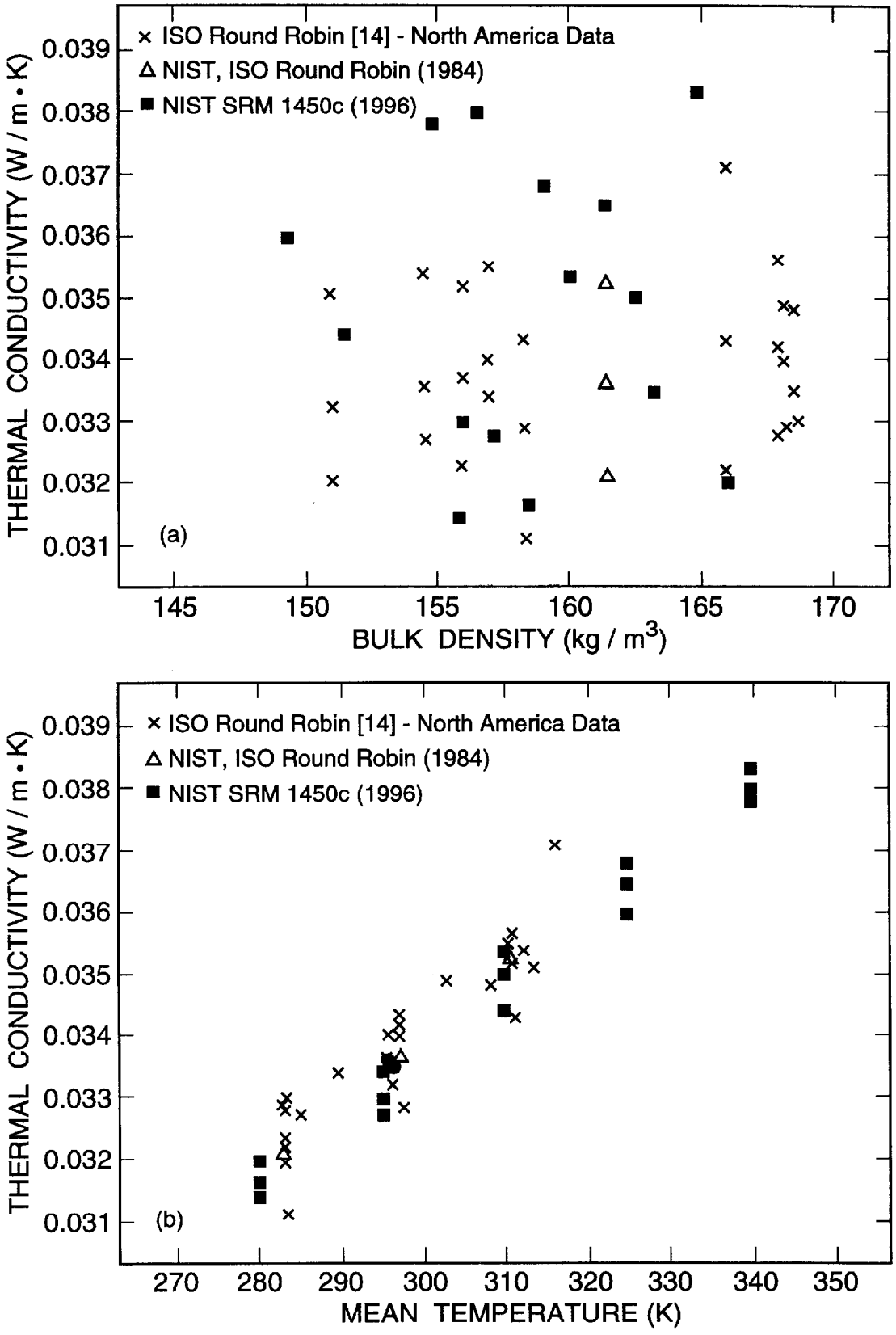


Figure 15. Comparison of data from SRM1450c and the ISO Round Robin [14].

Figure 16 plots predicted values of thermal conductivity for $\rho = 160$ kg/m$^3$ as a function of mean temperature for the ISO Round Robin and the SRM 1450 Series. The differences between predicted values for SRM 1450c and predicted values for the other lots of materials are illustrated in Figure 17. In general, the differences between predicted values for SRM 1450c and 1450, 1450a, and the ISO Round Robin were less than 2 percent; for 1450b, less than 7 percent. The major source for the differences can most likely be attributed to variations among the different lots of materials. For example, Hust [4] previously attributed the difference noted in predicted values for SRM 1450b to a variation in binder content and possible variations in fiber diameter and orientation. Further work is required to determine variations due to different test equipment or operator effects.

## 9. Certified Values of Thermal Resistance

Certified values of thermal resistance ($\hat{R}$) for SRM 1450c were calculated for a (hypothetical) 25.4-mm-thick specimen using the following equation:

$$\hat{R} = \frac{L}{\hat{\lambda}}. \qquad \textbf{(8)}$$

Predicted values of thermal conductivity ($\hat{\lambda}$) were computed from Equation (5). The value of 25.4 mm for L was selected to be consistent with the SRM 1450 Series. Certified values of $\hat{R}$ and expanded uncertainties, as defined below, are given in Table 8 for bulk density and mean temperature ranging from 150 kg/m$^3$ to 165 kg/m$^3$, and 280 K to 340 K, respectively.

**Table 8**
**Certified Values of Thermal Resistance (in m$^2$·K/W) of 25.4 mm Thick Specimen**

| Temperature (K) | Bulk Density (kg/m$^3$) | | | |
|---|---|---|---|---|
| | **150** | **155** | **160** | **165** |
| **280** | 0.818 ± 0.013 | 0.810 ± 0.013 | 0.803 ± 0.013 | 0.796 ± 0.012 |
| **285** | 0.804 ± 0.013 | 0.797 ± 0.012 | 0.790 ± 0.012 | 0.783 ± 0.012 |
| **290** | 0.790 ± 0.012 | 0.783 ± 0.012 | 0.777 ± 0.012 | 0.770 ± 0.012 |
| **295** | 0.777 ± 0.012 | 0.770 ± 0.012 | 0.764 ± 0.011 | 0.757 ± 0.011 |
| **300** | 0.764 ± 0.011 | 0.758 ± 0.011 | 0.752 ± 0.011 | 0.745 ± 0.011 |
| **305** | 0.752 ± 0.011 | 0.746 ± 0.011 | 0.740 ± 0.011 | 0.734 ± 0.011 |
| **310** | 0.740 ± 0.011 | 0.734 ± 0.011 | 0.728 ± 0.010 | 0.722 ± 0.010 |
| **315** | 0.729 ± 0.010 | 0.723 ± 0.010 | 0.717 ± 0.010 | 0.711 ± 0.010 |
| **320** | 0.717 ± 0.010 | 0.712 ± 0.010 | 0.706 ± 0.010 | 0.701 ± 0.010 |
| **325** | 0.707 ± 0.010 | 0.701 ± 0.010 | 0.696 ± 0.009 | 0.690 ± 0.009 |
| **330** | 0.696 ± 0.009 | 0.691 ± 0.009 | 0.686 ± 0.009 | 0.680 ± 0.009 |
| **335** | 0.686 ± 0.009 | 0.681 ± 0.009 | 0.676 ± 0.009 | 0.671 ± 0.009 |
| **340** | 0.676 ± 0.009 | 0.671 ± 0.009 | 0.666 ± 0.009 | 0.661 ± 0.009 |

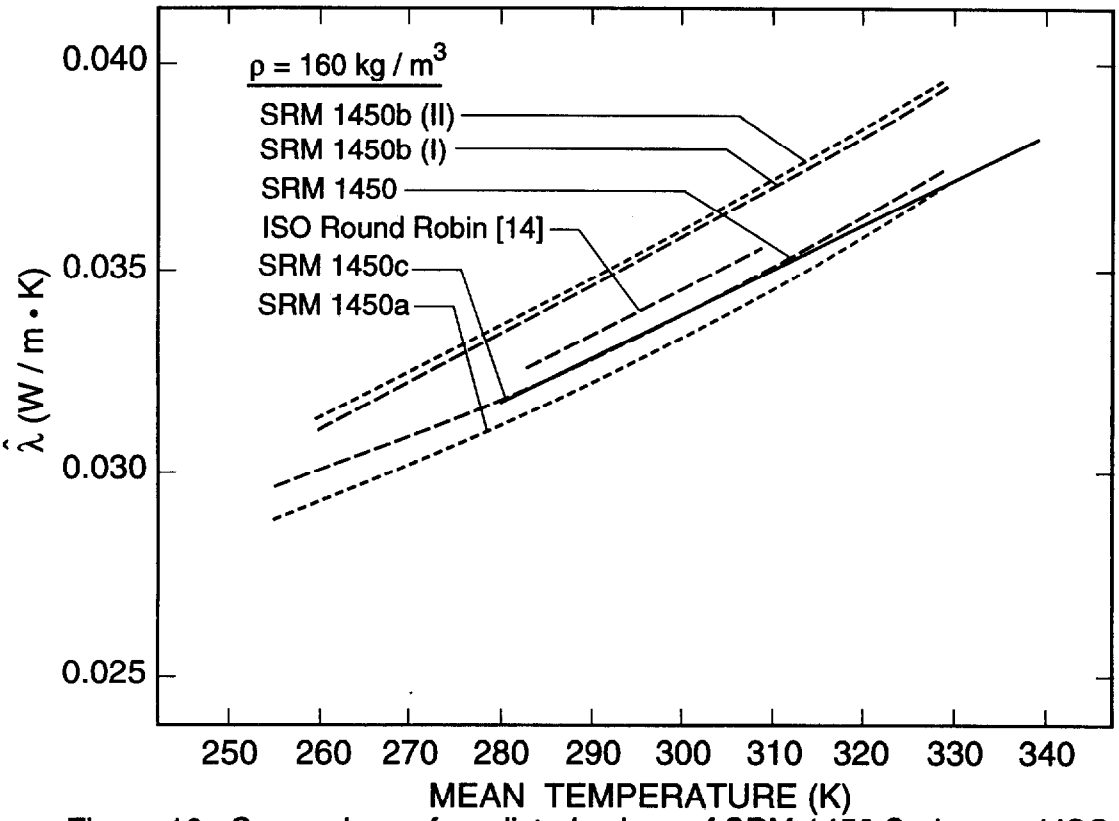


Figure 16. Comparison of predicted values of SRM 1450 Series and ISO Round Robin.

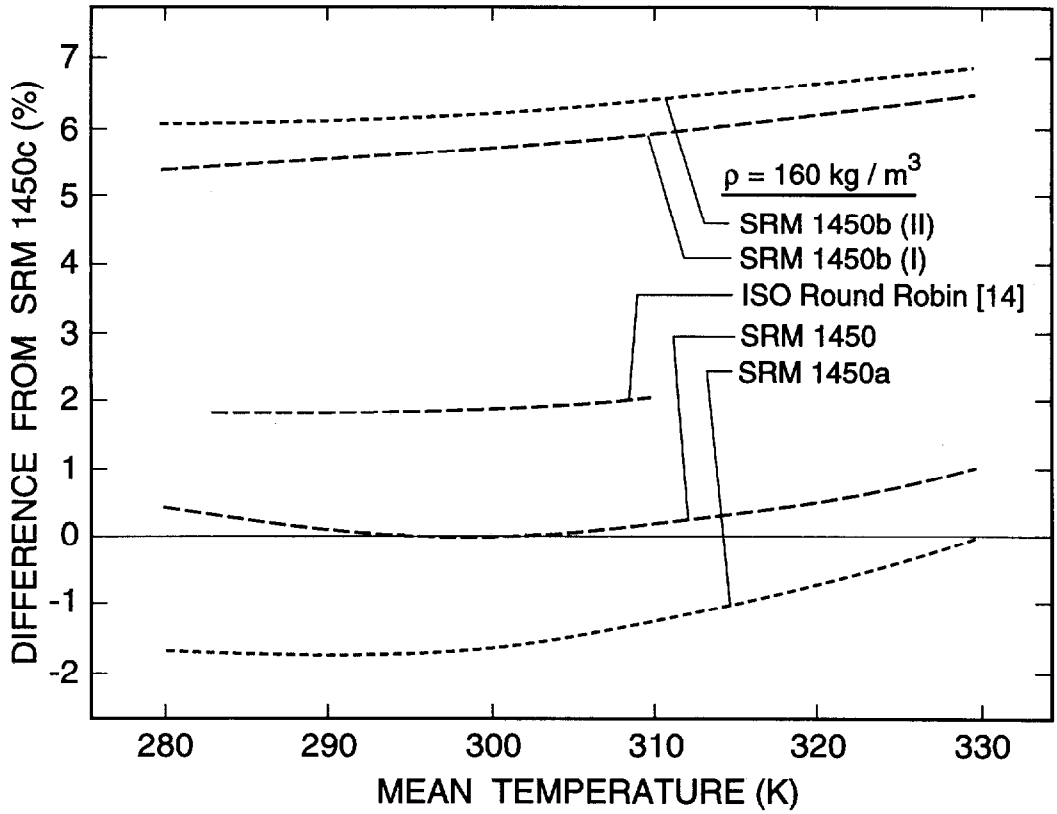


Figure 17. Comparison of predicted values of SRM 1450 Series and ISO Round Robin with respect to predicted values of SRM 1450c ($\rho$ = 160 kg/m$^3$).

***Restrictions and Precautions***

The certified values of $\hat{R}$ in Table 8 are restricted to the measured ranges of bulk density, mean temperature, thickness, and thermal conductivity presented herein. This means that certified values of $\hat{R}$ are valid only over the density range of 150 kg/m$^3$ to 165 kg/m$^3$, the temperature range of 280 K to 340 K, and the thickness range of 24.9 mm to 25.6 mm, which was based on two times the standard deviation of the thickness data in Table 6. Certified values of $\hat{R}$ are *not* valid when specimens of SRM 1450c have been stacked to increase thickness; that is $L$»25.4 mm or, for that matter, $L$«25.4 mm. As a final note, the boundary conditions of the user application must be comparable to the (normal) emissivity, ε, of the plate surfaces of the NIST guarded hot plate apparatus, ε = 0.89.

With reasonable care, specimens of SRM 1450c should have an indefinite shelf life. The material is only slightly sensitive to humidity and may be stored at laboratory conditions of approximately 21°C and a relative humidity, up to 50 percent. For thermal testing, specimens must be in firm contact with the apparatus plates but should not be compressed more than 2.5 mm (10 percent) of their original thickness. The upper temperature of use for SRM 1450c is limited to the decomposition point of the phenolic binder, approximately 200 °C (473 K). A lower temperature limit for SRM 1450c has not been established, but there is no known lower limit, in principle. The effect due to changes in ambient atmospheric pressure is negligible as noted by Smith and Hust [15] for a similar fibrous-glass material.

***Uncertainty***

The expanded uncertainty, $U$, for predicted values of $\hat{\lambda}$ was obtained by multiplying the combined standard uncertainty for predicted values of $\hat{\lambda}$, $u_c(\hat{\lambda})$ by a coverage factor of $k = 2$:

$$U(\hat{\lambda}) = k u_c(\hat{\lambda}). \qquad \textbf{(9)}$$

The combined standard uncertainty, $u_c(\hat{\lambda})$ was determined from the individual contributions of: (1) the standard uncertainty for the regression analysis for $\hat{\lambda}$; (2) the standard uncertainty for the measurement of λ; and, (3) the standard uncertainties for the measurements of ρ and $T$. The conservative estimate for the standard uncertainty for the regression analysis was 0.00014 W/(m⋅K) (Section 8) and the standard uncertainty for the measurement of λ was 0.00020 W/(m⋅K) as described in Appendix B. The standard uncertainties for the measurements of ρ and $T$ were 0.72 kg/m$^3$ (Appendix C) and 0.034 K (Appendix B), respectively, which were propagated in eq (5) to yield a standard uncertainty of 0.00004 W/(m⋅K). These individual contributions were combined to yield a combined standard uncertainty $u_c(\hat{\lambda})$ of 0.00025 W/(m⋅K) ($k$ = 1). Therefore, the expanded uncertainty for predicted values of $\hat{\lambda}$ was 0.00050 W/(m⋅K) ($k$ = 2). This estimate does not include any estimates for uncertainties introduced by the user or long-term drifts in the material.

The expanded uncertainties, $U$, for certified values of $\hat{R}$ in Table 8 were based on the following equation:

$$U(\hat{R}) = k u_c(\hat{R}) = k\sqrt{c_{\hat{\lambda}}^2 u_c^2(\hat{\lambda})}, \qquad \textbf{(10)}$$

where the sensitivity coefficient $c_{\hat{\lambda}} = -(0.0254/\hat{\lambda}^2)$ and $u_c(\hat{\lambda})$ was obtained from eq (9). Note that the sensitivity coefficient $c_{\hat{\lambda}}$ varies with $\hat{\lambda}$ and therefore the standard uncertainties for $\hat{R}$ also vary, as noted in Table 8. Consequently, the values of expanded uncertainty quoted in Table 8 are valid only for the given hypothetical thickness of 25.4 mm (1 in.). The maximum expanded uncertainty for $\hat{R}$ in Table 8 is ± 0.013 $m^2 \cdot K/W$ ($k = 2$) at 150 $kg/m^3$ and 280 K, which, in relative terms, is ±1.6 percent. This value of relative expanded uncertainty compares quite well to the previous published uncertainty values of ± 2 percent for SRM 1450b [4].

## 10. Summary and Conclusions

Thermal conductivity measurements at room temperature are presented as the basis for certified values of thermal resistance for SRM 1450c, Fibrous Glass Board. The thermal conductivity measurements were conducted over ranges of bulk density from 150 $kg/m^3$ to 165 $kg/m^3$ and mean temperatures from 280 K to 340 K using NIST's one-meter guarded-hot-plate apparatus. A model dependent on these two parameters has been developed that describes the thermal conductivity over the range of the parameters. An expanded uncertainty, consistent in format with current international guidelines, has been prepared for predicted values of thermal conductivity and certified values of thermal resistance. Material characterization of the material revealed local (within-board) variations of bulk density ranging about 11 percent. This variation should not affect the "average" thermal conductivity of a specimen by more than 1 percent. The source of local (within-board) variations of bulk density was believed due, in part, to variations in application of the fiber's phenolic binder as well as variations in the distribution of the glass fibers. Further research is recommended to determine the source of local variations of bulk density. Comparison of predicted values of thermal conductivity for SRM 1450c agreed to within 2 percent of the North American results of an international round robin and within less than 1 percent to 7 percent of predicted values for previous material lots of the SRM 1450 Series. The differences were believed primarily due to material variations among the lots of materials.

## 11. Acknowledgments

The authors acknowledge the contributions of several people: Robert Gettings, who provided support through the Standard Reference Materials Program; and NIST Statistician, Dr. Eric Lagergren, who provided guidance in the experimental design and data analysis. Thermal conductivity measurements were obtained with the assistance of Erik H. Anderson, and imbalance tests were conducted with the assistance of Mark W. Davis. Compressive resistance measurements were provided by Dr. Walter J. Rossiter and Kevin M. Kraft, and SEM micrographs were filmed by Paul E. Stutzman. Thermogravimetry measurements were provided by Dr. Barry J. Bauer.

## 12. References


[1] Taylor, J.K. "Standard Reference Materials, Handbook for SRM Users," *NIST Special Publication 260-100*, February 1993, p.26.

[2] Siu, M.C.I. "Fibrous Glass Board as a Standard Reference Material for Thermal Resistance Measurement Systems," *Thermal Insulation Performance, ASTM STP 718*, D.L. McElroy and R.P. Tye, Eds., American Society for Testing and Materials, Philadelphia, 1980, pp. 343-360.

[3] ASTM Subcommittee C-16.30. "Reference Materials for Insulation Measurement Comparisons," *Thermal Transmission Measurements of Insulation, ASTM STP 660*, R.P. Tye, Ed., American Society for Testing and Materials, Philadelphia, 1978, pp. 7-29.

[4] Hust, J.G. "Standard Reference Materials: Glass Fiberboard SRM for Thermal Resistance," *NBS Special Publication 260-98*, August 1985.

[5] Grimes J.T. "Evaluation of National Institute of Standards and Technology (NIST) Thermal Conductivity Standard Reference Materials Using a 20-cm Heat Flow Meter Apparatus," *Journal of Thermal Insulation*, Vol. 13, 1989, pp. 62-70.

[6] Mumaw, J.R. Owens Corning, 1996, private communication.

[7] ASTM C 165. "Standard Test Method for Measuring Compressive Properties of Thermal Insulation," *Annual Book of ASTM Standards, Vol. 04.06*.

[8] Burch, D.M. and A.O. Desjarlais. "Water-Vapor Measurements of Low-Slope Roofing Materials," *NISTIR 5681*, July 1995.

[9] ASTM C 177. "Standard Test Method for Steady-State Heat Flux Measurements and Thermal Transmission Properties by Means of the Guarded Hot Plate Apparatus," *Annual Book of ASTM Standards, Vol. 04.06*.

[10] Powell, F.J. and B.G. Rennex. "The NBS Line-Heat-Source Guarded Hot Plate for Thick Materials," *Thermal Performance of the Exterior Envelopes of Buildings - II, ASHRAE SP 38*, 1983, pp. 657-672.

[11] Zarr, R.R. and M.H. Hahn. "Line Heat Source Guarded Hot Plate Apparatus: Adjunct ASTM Practice C 1043," *Annual Book of ASTM Standards, Vol. 04.06*.

[12] ISO. *Guide to the Expression of Uncertainty in Measurement*, International Organization for Standardization, Geneva, Switzerland, 1993.

[13] Taylor, B.N. and C.E. Kuyatt. "Guidelines for Evaluating and Expressing the Uncertainty of NIST Measurement Results," *NIST Technical Note 1297*, 1994.

[14] Smith, D.R. "Apparent Thermal Conductivity of Fibrous Glass Board by Guarded Hot Plates and Heat Flow Meters: An International Round Robin," *Journal of Thermophysical Properties*

(in publication).

[15] Smith, D.R. and J.G. Hust. "Effective Thermal Conductivity of Glass-Fiber Board and Blanket Standard Reference Materials," *Thermal Conductivity 17*, J.G. Hust, Ed., 1983, p.491.

[16] Roark, R.J. *Formulas for Stress and Strain*, 4th Ed., 1965, p. 219.

**Appendix A**

**UNITED STATES DEPARTMENT OF COMMERCE**
**National Institute of Standards and Technology**
**Gaithersburg, Maryland 20899-0001**

**QUESTIONNAIRE ON SRM 1450c, FIBROUS-GLASS BOARD**

Date of Purchase: __/__/__

To better serve you, we ask that you take a few moments to fill out the short questionnaire below.
***When finished, please fax this questionnaire to Robert R. Zarr at (301) 990-4192, or fold and mail no later than September 15, 1995.***
Please tell us...

**... about your Company:**
Company's name: _____
Address: _____
Primary business activity: _____
User's telephone numbers; voice: (____) ____ - _____ fax: (____) ____ - _____

**... about your measurement process (check appropriate box):**
Your measurement application(s): _____
ASTM Test Method: ‘ C 177 ‘ C 518 ‘ Other: _____
Instrument(s) used (model): _____
Maximum uncertainty acceptable in your measurement process(es)
‘ <10% ‘ <5% ‘ <2% ‘ <1% ‘ Other: _____
Specimen size required: _____
Specimen thicknesses required: _____
Temperature range required for measurement process: _____

**... about the requirements you would like for SRM 1450c:**
Size: ‘ 610 x 610 mm ‘ Other: _____ Thickness: ‘ 25.4 mm ‘ Other: _____
What temperature range do you require: _____
(Note: the greater the range, the higher the cost)
How quickly do you need SRM 1450c:
‘ 5 Years ‘ 2 Years ‘ 1Year ‘ Other: _____
Would you like the same nominal density and thermal conductivity:
‘ Yes ‘ No, I prefer _____
Should the material be from the same manufacturer as previous lots: ‘ Yes ‘ No
Comments: _____

**... any additional comments:** _____
_____
_____
_____

Thank you for your prompt reply. Your answers will help us to better serve your SRM needs. If you have technical questions, please contact Robert R. Zarr at e-mail chat@enh.nist.gov.

| Table A1<br>List of Individuals, Company, or Organization Responding to SRMP Questionnaire (433 mailed) | | |
|---|---|---|
| 1 | AEL ISD MO. | 1 |
| 2 | Anacon Corporation | 1 |
| 3 | Arizona State University | 1 |
| 4 | Bayer Corporation | 1 |
| 5 | Carborundum-Fibers Division | 1 |
| 6 | Cell-U-Foam Corporation | 1 |
| 7 | Celotex Corporation | 1 |
| 8 | Celotex Ltd. | 1 |
| 9 | Center for Applied Engineering, Inc. | 1 |
| 10 | Childers Product Company | 1 |
| 11 | ConsultMort, Inc. | 1 |
| 12 | Consumers Power Company | 1 |
| 13 | CTL | 1 |
| 14 | David L. McElroy | 1 |
| 15 | Dow Chemical R&D | 1 |
| 16 | Exeltherm, Inc. | 1 |
| 17 | Forest Products Labs | 1 |
| 18 | GAF Materials Corporation | 1 |
| 19 | Holometrix | 1 |
| 20 | Huntsman Corporation | 1 |
| 21 | ICI Polyurethanes | 1 |
| 22 | IFC Kaiser Engineers/ INEL Tank Farm Project | 1 |
| 23 | IMI-Tech Corporation | 1 |
| 24 | Instafoam Products | 1 |
| 25 | Knauf | 1 |
| 26 | Korea Research Institute of Standards and Science | 1 |
| 27 | Lamolite, Inc. | 1 |
| 28 | LaserComp | 1 |
| 29 | Owens Corning | 7* |
| 30 | Pabco | 1 |
| 31 | Phillips Petroleum Company | 1 |
| 32 | Pittsburgh Corning | 1 |
| 33 | Rockwool, International | 1 |
| 34 | Rollin Incorporated | 1 |
| 35 | R&D Services, Inc. | 1 |
| 36 | TNO Building and Construction Research | 1 |
| 37 | UC Industries | 1 |
| 38 | Underwriters Lab, Inc. | 1 |
| 39 | Volberg Insulation, Inc. | 1 |
| 40 | Wiss, Janney, Elstner and Associates, Inc. | 1 |

* Only two returns counted

## Appendix B

## Uncertainty Analysis for Thermal Conductivity (λ)

### *Background*

In 1992, NIST officially adopted a new policy [12] for the expression of measurement uncertainty consistent with international practices set forth in the ISO *Guide to the Expression of Uncertainty in Measurement* [13]. This policy provides a uniform approach at NIST to uncertainty analysis and is summarized briefly below. Further details are available in references [12,13].

In many cases, a measurand $Y$ is not determined directly from a single measurement, but rather mathematically from a function of $N$ other *independent* quantities $X_i$:

$$Y = f(X_1, X_2, ..., X_N). \qquad \textbf{(B-1)}$$

The output estimate of $Y$, denoted as $y$, is obtained using input estimates $x_i$ for the values of the $N$ independent quantities $X_i$:

$$y = f(x_1, x_2, ... x_N). \qquad \textbf{(B-2)}$$

The combined standard uncertainty of $y$, $u_c(y)$, is the positive square root of the combined variance, $u_c^2(y)$; where

$$u_c^2(y) = \sum_{i=1}^{N} \left( \frac{\partial f}{\partial x_i} \right)^2 u^2(x_i) = \sum_{i=1}^{N} c_i^2 u^2(x_i). \qquad \textbf{(B-3)}$$

Equation (B-3) is commonly referred to as the "law of propagation of uncertainty." The partial derivatives are known as sensitivity coefficients ($c_i$) and are equal to $\partial f/\partial X_i$ evaluated at $X_i = x_i$. The corresponding term, $u(x_i)$, is the standard uncertainty associated with the input estimate $x_i$.

Each $u(x_i)$ is evaluated as either a Type A or a Type B standard uncertainty. Type A standard uncertainties are evaluated by statistical means. Type B standard uncertainties cannot be determined directly from the experiment at hand and must be evaluated by other means, such as (previous) measurement data from another experiment, experience, a calibration certificate, manufacturer's specification, etc. [12,13]. Categorizing the evaluation of uncertainties as Type A or Type B is simply a matter of convenience, since both are based on probability distributions[3] and combined equivalently in eq (B-3). An example of a Type A evaluation is provided below. Examples of Type B evaluations are provided in references [12,13]. It should be noted that the designations "A" and "B" apply to the two methods of evaluation, not the type of error. In other words, the designations "A" and "B" have nothing to do with the traditional terms "random" or "systematic."

---

[3] This is not entirely true. The probability distribution for a Type B evaluation, as opposed to a Type A evaluation, is assumed based on the experimenter's judgement.

As an example of a Type A evaluation, consider an input quantity $X_i$ determined from $n$ independent observations obtained under the same conditions (i.e., repeated observations). In this case, the input estimate $x_i$ is the sample mean determined from

$$x_i = \overline{X}_i = \frac{1}{n} \sum_{k=1}^{n} X_{i,k}. \qquad \textbf{(B-4)}$$

The standard uncertainty, $u(x_i)$ associated with $x_i$ is the estimated standard deviation of the sample mean:

$$u(x_i) = s(\overline{X}_i) = \frac{s}{\sqrt{n}}. \qquad \textbf{(B-5)}$$

When an additional level of uncertainty is required that provides an interval (similar to a confidence interval, for example), an expanded uncertainty, $U$, is obtained by multiplying the combined standard uncertainty, $u_c(y)$, by a coverage factor, $k$:

$$U = k u_c(y) = k\sqrt{\sum c_i^2 u^2(x_i)_A + \sum c_i^2 u^2(x_i)_B}. \qquad \textbf{(B-6)}$$

The value of $k$ is chosen based on the desired level of confidence to be associated with the interval defined by $U$ and typically ranges from 2 to 3. Interpretation of the coverage factor requires a word of caution. The term "confidence interval" has a specific definition in statistics and is applicable only to intervals based on $u_c$ when certain conditions are satisfied, including that *all* components of $u_c$ be obtained from Type A evaluations. Under these circumstances, a coverage factor of $k = 2$ defines an interval having a level of confidence of about 95 percent and $k = 3$ defines an interval having a level of confidence greater than 99 percent. At NIST, the value of the coverage factor is $k = 2$, by convention [13].

***Components of Uncertainty for λ***

Referring to eq (2) in the text, the standard uncertainty for measured values of λ was evaluated based on the individual standard uncertainties for the specimen heat flow ($Q$), meter area ($A$), in-situ thickness ($L$), and specimen temperature difference, ($\Delta T$). These individual standard uncertainties were evaluated by either statistical methods (Type A), other means (Type B), or both, and are discussed below.

***Specimen Heat Flow (Q)***

Under normal operation (see Figure 12 in the text), the guard plate and ambient air temperature were maintained such that lateral heat losses ($Q_{gap}$ and $Q_{edge}$) were reduced to negligible proportions in comparison to the specimen heat flow ($Q$). Under these circumstances, $Q$ was determined by simply measuring the DC electrical power provided to the meter area ($Q_m$) of the guarded hot plate. The electrical circuit for the measurement consisted of a standard resistor, nominally 0.1 Ω, in series with the electrical heater of the meter area, as illustrated in Figure B1. The corresponding equation for the power input to the meter area is:

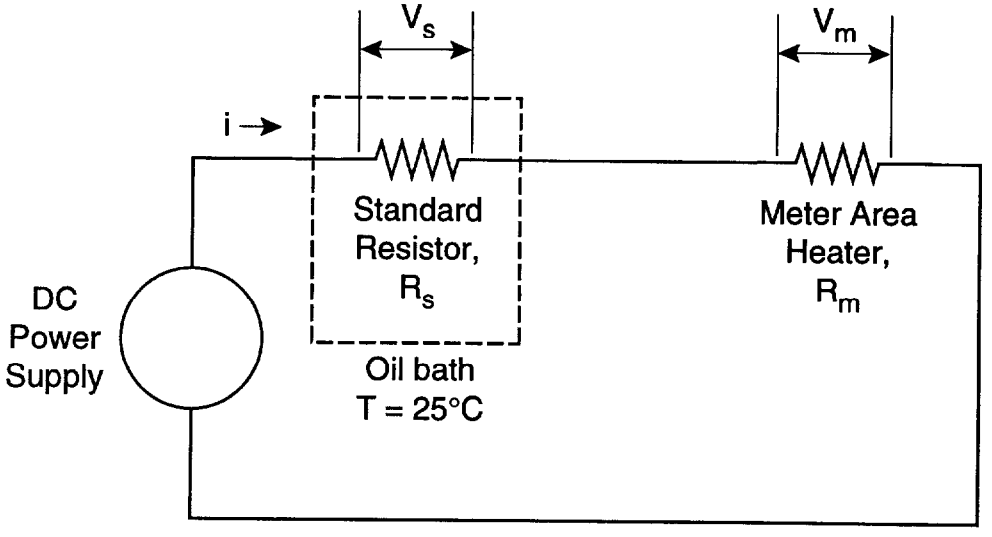


Figure B1. Electrical circuit for measurement of power to the meter area.

$$Q_m = i V_m = \left( \frac{V_s}{R_s} \right) V_m, \qquad \textbf{(B-7)}$$

where $i$ is the current ($V_s/R_s$) measured at the standard resistor, and $V_m$ is the voltage drop measured across the electrical leads to the meter area. For these tests, $Q$ was approximately 3.6 W.

The Type A and Type B standard uncertainties for the determination of the specimen heat flow ($Q$) are summarized in Table B-1. The Type A standard uncertainty for the repeated power measurements was determined by pooling the standard deviations for each guarded hot plate test. The Type A standard uncertainties for the voltage measurements were determined by regression analysis of calibration data. The Type B standard uncertainties for the voltage measurements were assumed to have a uniform distribution in the interval 2$a$, where $a$ was determined from the manufacturer's specification for the integrating digital voltmeter (DVM). The intervals 2$a$ for the digital voltmeter for the 30-V and 300-mV ranges were 4.11 mV and 12.7 µV, respectively.

**Table B-1**
**Uncertainty Budget: Specimen Heat Flow (Q)**

| Source of Uncertainty | Standard Uncertainty $u(x_i)$ and Type | Degrees of Freedom (A) or Source (B) |
|---|---|---|
| 1) Repeated test measurements | 0.00054 W (A) | DF = 1785 |
| 2) Voltage measurement ($V_m$):<br>- calibration DVM, 30V<br>- uncertainty DVM, 30V | <br>0.000003 V (A)<br>0.002370 V (B) | <br>DF = 20<br>Manufacturer, $u(V_{m2}) = a/\sqrt{3}$ |
| 3) Current determination (I):<br>- std. resistor ($R_s$) calibration<br>- calibration DVM, 300 mV<br>- uncertainty DVM, 300 mV | <br>0.000001 Ω (B)<br>0.000009 V (A)<br>0.000007 V (B) | <br>NIST Calibration (k = 1)<br>DF = 20<br>Manufacturer, $u(V_{s3}) = a/\sqrt{3}$ |
| 4) Imbalance effects ($Q_g$) | 0.0098 W (B) | Experiment, Appendix B |

### *Guard Imbalance ($Q_g$)*

The term $Q_g$ in Table B-1 represents both the lateral heat loss at the guard gap between the meter and guard plates ($Q_{gap}$) and the heat loss at the edges of the specimens ($Q_{edge}$). Typically, $Q_g$ was quite small (approximately zero) for the 15 guarded hot plate tests because guarding at the gap and edges of the specimen reduced the lateral heat flows $Q_{gap}$ and $Q_{edge}$ to negligible proportions, Figure 12. An imbalance results when a temperature difference develops either across the gap ($V_{gap}$) or at the edge of the specimens ($T_a$-$T$). In our case, $V_{gap}$ and $T_a$-$T$ refer to the voltage outputs from a 8-junction Type-E thermopile across the gap, and the temperature difference between the ambient air and mean temperature, respectively. An estimate for the Type B standard uncertainty of $Q_g$ was determined from an extensive experimental effort described below.

Fifteen tests were conducted with a single pair of specimens of fibrous glass boards (051 and 118) at mean temperatures ($T$) of 280 K, 310 K, and 340 K. The specimens were installed in the guarded-hot-plate apparatus following the same procedures as previous tests. At each mean temperature, five tests were conducted in random sequence with $V_{gap}$ and $T_a$ -$T$ varied at two levels, Figure B2. The experimental design also included a center point where $V_{gap}$ and $T_a$ -$T$ were both set to zero; that is, normal operating conditions for negligible heat flows at the guard gap and specimen edges. This experimental design allowed us to check our previous results and any interaction between the independent quantities.

During each test, the steady-state power input to the meter plate ( $Q_m$) was recorded and averaged for the test. The guard imbalance, $Q_g$, was defined as

$$Q_g = Q_m - Q_{m_0}. \qquad \textbf{(B-8)}$$

where $Q_{m_o}$ was the power input to the meter plate for the gap and edge temperatures thermally balanced, i.e., at the center point where $Q_g$ = zero and $Q_m = Q_{m_o} - 3.6$ W. The data for $Q_m$-$Q_{m_o}$ versus $V_{gap}$ and $T_a$- $T$ are plotted in Figures B3a and B3b, respectively. The change in the power input to the meter plate was quite sensitive to change in $V_{gap}$ and less sensitive to an imbalance for $T_a$ - $T$. A change of ± 50 μV in $V_{gap}$ caused an error of ± 0.1 W in the power input to the meter plate; a change of ± 4 K in $T_a$ - $T$ caused a change of about ± 0.01 W. The effect of mean temperature was small, as observed in Figures B3a and B3b, and the effect of the independent variables on each other was, for the most part, uncorrelated. That is, there was no interaction between $V_{gap}$ and $T_a$ - $T$.

The data in Figures B3a and B3b were fit to a linear model in $V_{gap}$ and $T_a$ - $T$ at mean temperatures of 280 K, 310 K, and 340 K:

$$Q_m - Q_{m_0} = b_0 + b_1 V_g + b_2 (T_a - T). \qquad \textbf{(B-9)}$$

The coefficients, $b_0$, $b_1$, and $b_2$ were determined by multiple variable linear regression, Table B-2. Based on experimental judgement, a conservative estimate for the Type B standard uncertainty for $Q_g$ (Table B-1) was determined at 310 K for a gap imbalance of 2.5 μV (0.01 K) and an imbalance in ambient temperature of 0.5 K.

**Table B-2**
**Regression Coefficients for Guard Gap and Ambient Temperature Imbalance**

| T (K) | $b_0$ (W) | $b_1$ (W/μV) | $b_2$ (W/K) | RSD* (W) |
|---|---|---|---|---|
| 280 | $2.988\times10^{-3}$ | $2.323\times10^{-3}$ | $2.416\times10^{-3}$ | 0.0028 |
| 310 | $2.422\times10^{-3}$ | $2.547\times10^{-3}$ | $1.921\times10^{-3}$ | 0.0044 |
| 340 | $-2.724\times10^{-4}$ | $2.607\times10^{-3}$ | $-6.939\times10^{-3}$ | 0.0057 |

*Residual standard deviation

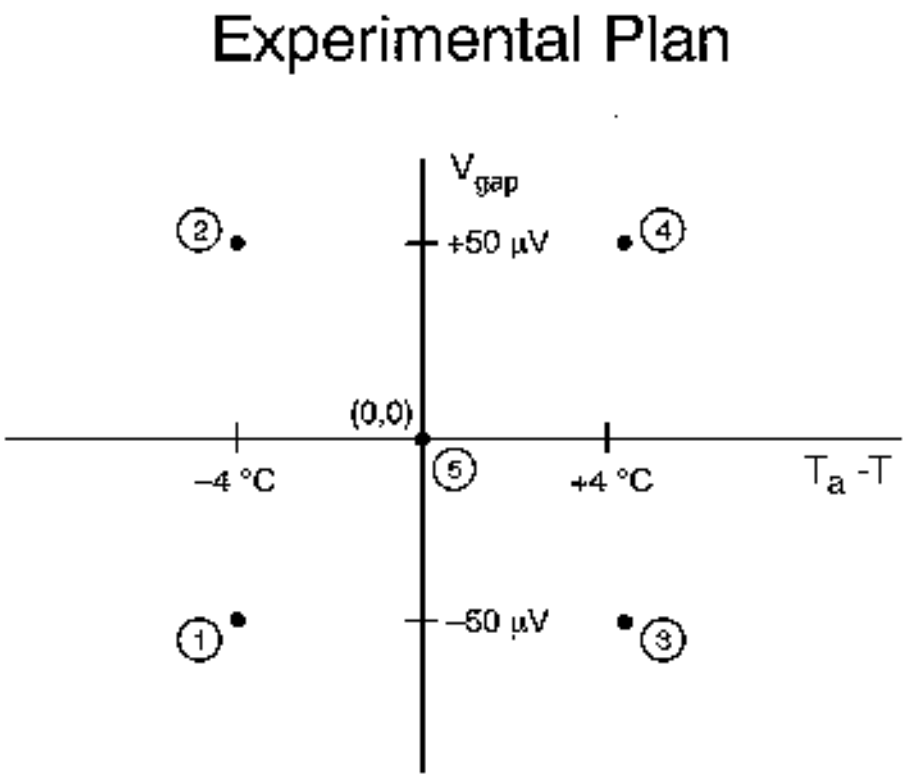


Figure B2. Experimental design for guard gap imbalance and ambient temperature imbalance.

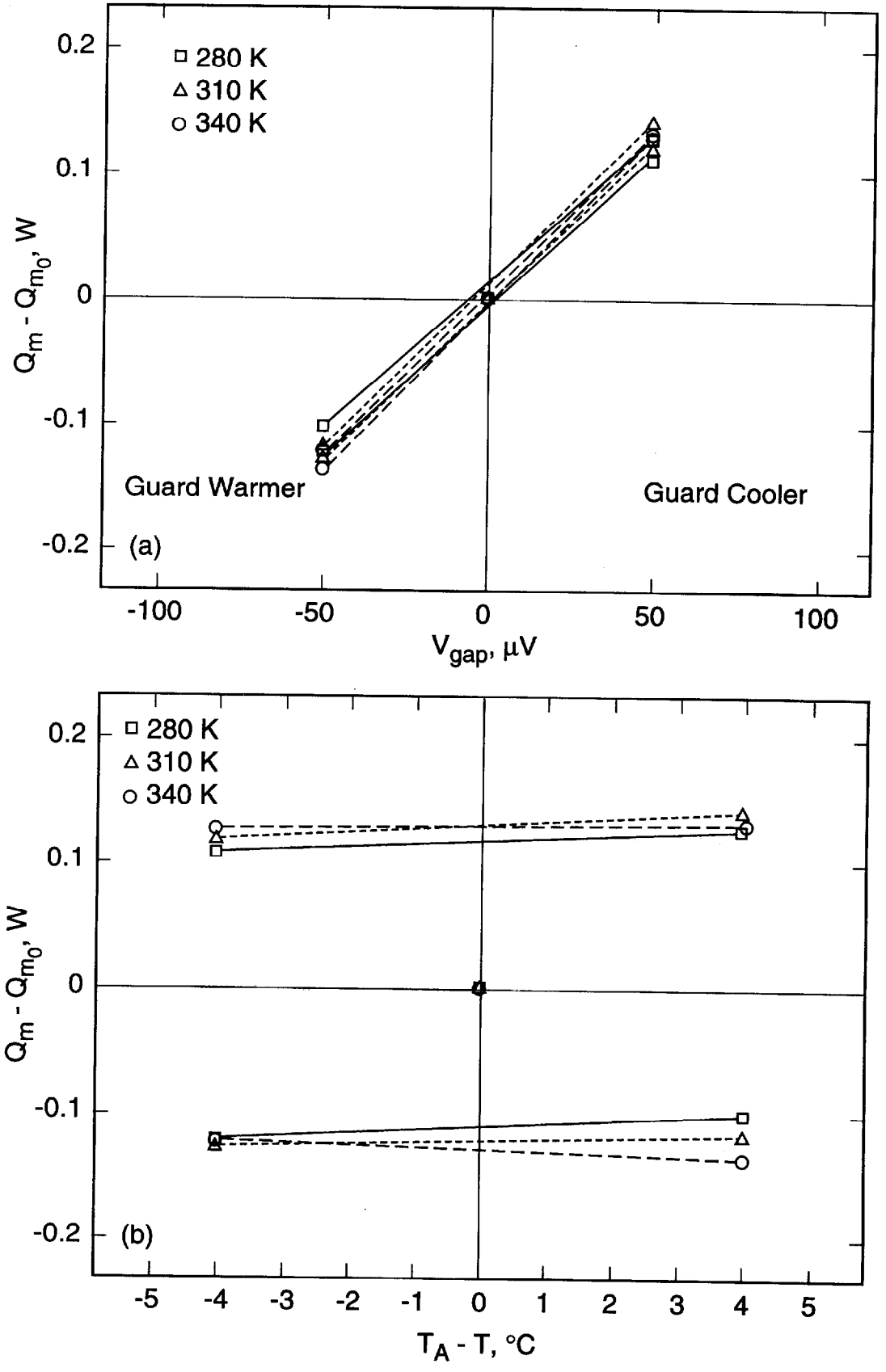


Figure B3. (a) Effect of guard gap imbalance on meter plate power.
(b) Effect of ambient imbalance on meter plate power.

The combined standard uncertainty for $Q$ was determined from the application of eq (B-3), resulting in the following expression:

$$u_c^2(Q) = c_{Vs}^2 u^2(V_s) + c_{Rs}^2 u^2(R_s) + c_{Vm}^2 u^2(V_m) + c_{Qg}^2 u^2(Q_g), \quad \textbf{(B-10)}$$

where

$c_{Vs} = \partial Q/\partial V_s = V_m/R_s$,
$c_{Rs} = \partial Q/\partial R_s = -(V_s/R_s^2)V_m$,
$c_{Vm} = V_s/R_S = i$, and
$c_{Qg} = \partial Q/\partial Q_g = 1$.

The standard uncertainties for Equation (B-10) were taken from Table B-1. Evaluation of eq (B-10) yielded a combined standard uncertainty for $Q$ of 0.0101 W or in relative terms, 0.28 percent.

***Meter Area (A)***

The meter area is the mathematical area through which the heat input to the meter plate flows normally under ideal guarding conditions (i.e., $Q_g = 0$) into the specimen. The meter area was calculated from the equation:

$$A = \pi r^2 = \frac{\pi}{2}(r_o^2 + r_i^2)(1 + \alpha\Delta T_{mp})^2, \quad \textbf{(B-11)}$$

where

$r_o$ = outer radius of meter plate, m
$r_i$ = inner radius of guard plate, m
$\alpha$ = coefficient of thermal expansion of meter plate, $K^{-1}$ and
$\Delta T_{mp}$ = temperature difference, K.

The values for $r_o$ and $r_i$ were 0.2028 m and 0.2036 m (7.985 in. and 8.015 in.), respectively, and a value of $2.36\times10^{-5}$ $K^{-1}$ for $\alpha$ was taken from handbook data for aluminum alloy 6061-T6. The maximum value for $\Delta T_{mp}$ was 57 K, which was computed for a mean temperature of 340 K. The combined standard uncertainty was determined to be $4.184\times10^{-5}$ $m^2$ (relative standard uncertainty of 0.032 percent), which includes the individual (standard) uncertainty contributions for $r_o$, $r_i$, $\alpha$, and $\Delta T_{mp}$.

***In-situ Thickness (L)***

The thickness of each pair of specimens was measured during testing using the average of eight (four top and four bottom) linear positioning transducers equally spaced at the periphery of the plates. The corresponding equation for the in-situ thickness measurement is

$$L = \frac{\sum_{i=1}^{n} L_i}{n}, \qquad \textbf{(B-12)}$$

where $L_i$ is the measurement value for an individual transducer and $n = 8$. Each transducer consisted of a 450-mm Invar scale and slider, and digital indicator. In operation, the slider tracked the distance between the translating cold plate and the fixed guarded hot plate, and the corresponding output signal was displayed by the digital indicator with a resolution of $2.54 \times 10^{-6}$ m. The digital indicators were reset by placing four fused-quartz (96 percent) spacers of known thickness between the hot plate and cold plate at the same peripheral locations corresponding to the linear positioning transducers. Fused quartz was selected for the spacers because of its extremely low coefficient of thermal expansion, $5.5 \times 10^{-7}$ cm/(cm⇳K).

The Type A and Type B standard uncertainties for the determination of $L$ are summarized in Table B-3. The Type A standard uncertainty for the multiple locations was determined by pooling the standard deviations for each guarded hot plate test. The Type A standard uncertainty for the fused-quartz spacers was determined by taking the square root of the sum of the individual variances ($s^2$) for four thickness measurements of each quartz spacer. The Type A standard uncertainty for the calibration of the transducers was determined by repeated measurements in a separate experiment described below. The Type A standard uncertainty for the flatness of the meter plate was determined using an *xyz* coordinate measuring machine (CMM) having an uncertainty of 5.1 x $10^{-6}$ m. The thickness of the meter plate was measured at 32 different locations and the standard deviation of the 32 measurements was used in the Type A evaluation. The Type B standard uncertainties for the length measurements were assumed to have a uniform distribution in the interval 2$a$, where $a$ was the smallest length interval of the micrometer. The interval 2$a$ for the micrometer was 0.00254 mm. A Type B standard uncertainty for plate deflection was estimated for the large plates based on a classical deflection formula for a uniform load applied to a circular plate [16].

**Table B-3**
**Uncertainty Budget: Specimen Thickness (L)**

| Source of Uncertainty | Standard Uncertainty $u(x_i)$ and Type | Degrees of Freedom (A) or Source (B) |
|---|---|---|
| 1) Multiple locations | $8.79 \times 10^{-5}$ m (A) | DF = 105 |
| 2) System specification | $5.1 \times 10^{-6}$ m (B) | Manufacturer (k = 1, assumed) |
| 3) Fused-quartz spacers(4) cal.<br>- repeated measurements<br>- uncertainty of micrometer | <br>$1.14 \times 10^{-6}$ m (A)<br>$1.47 \times 10^{-6}$ m (B) | <br>DF = 12<br>$u(L_{3B}) = a/\sqrt{3}$ |
| 4) Calibration of transducers | $6.37 \times 10^{-6}$ m (A) | DF = 6.7 |
| 5) Plate flatness | $6.57 \times 10^{-6}$ m (A) | DF = 31 |

| Table B-3<br>Uncertainty Budget: Specimen Thickness (L) | | |
|---|---|---|
| 6) Plate deflection | $2.1\times10^{-5}$ m (B) | Calculation, Reference [16] |

The repeatability of the linear positioning transducers was determined from a series of replicate thickness measurements taken over several days using the fused-quartz spacers as reference values. The thickness transducers for the cold plates were initially reset using the four fused-quartz spacers and the cold plates were subsequently opened and closed until the plates were in complete contact again with all spacers. The readings from the digital indicators were recorded and the procedure was repeated five times. To check the variation from day-to-day, readings were taken over 4 days providing a total of 20 thickness averages. Table B-4 gives summary statistics for each day.

**Table B-4**
**Summary Statistics for Thickness Calibration**

| Day | Replicates | Day Averages (m) | Within-Day Std. Dev. (m) |
|---|---|---|---|
| 1 | 5 | $2.541 \times 10^{-2}$ | $3.96 \times 10^{-6}$ |
| 2 | 5 | $2.541 \times 10^{-2}$ | $4.28 \times 10^{-6}$ |
| 3 | 5 | $2.542 \times 10^{-2}$ | $3.29 \times 10^{-6}$ |
| 4 | 5 | $2.542 \times 10^{-2}$ | $2.54 \times 10^{-6}$ |

The standard deviation of the daily averages ($s_a$) was $5.12\times10^{-6}$ m and the (pooled) within-day standard deviation ($s_d$) was $4.24\times10^{-6}$ m. The standard uncertainty was determined to be $6.37\times10^{-6}$ m using Equation (B-13):

$$u(L_4) = \sqrt{(s_a)^2 + \frac{r-1}{r}(s_d)^2}, \qquad \textbf{(B-13)}$$

where $r$ = number of replicates per day. The DF (degrees of freedom) were determined from the Welch-Satterthwaite formula in Reference [13]. The combined standard uncertainty for thickness ($u_c(L)$) was determined to be $9.10\times10^{-5}$ m (relative standard uncertainty of 0.36 percent).

***Temperature Difference*** **($\Delta T$)**

The temperature difference of the specimens was determined from the following equation:

$$\Delta T = T_h - T_c = T_h - \tfrac{1}{2}(T_{c_1} + T_{c_2}), \qquad \textbf{(B-14)}$$

where the subscripts $h$ and $c$ refer to hot and cold, respectively, and the subscripts 1 and 2 refer to the two cold plates. The temperatures of the hot plate and cold plates were determined using

precision platinum resistance thermometers (PRTs). The electrical resistance of the PRTs was measured with an integrating DVM.

The Type A and Type B standard uncertainties for the determination of $\Delta T$ are summarized in Table B-5. The Type A standard uncertainty for the repeated temperature measurements was determined by pooling the standard deviations for each guarded hot plate test. The Type A standard uncertainty for the temperature determination was determined by regression analysis of calibration data provided by the NIST Thermometry Group. The Type B standard uncertainty for the resistance measurement was assumed to have a uniform distribution in the interval $2a$; where $a$ was determined from the manufacturer's specification for the integrating digital voltmeter (DVM). The interval $2a$ for the digital voltmeter for the 300-Ω range was 0.039 Ω. This standard uncertainty was probably overly conservative and contributed heavily to the combined standard uncertainty for λ. The combined standard uncertainty for temperature difference ($u_c(\Delta T)$) was determined to be 0.067 K (relative standard uncertainty of 0.34 percent).

**Table B-5**
**Uncertainty Budget: Temperature Difference (ΔT)**

| Source of Uncertainty | Standard Uncertainty $u(x_i)$ and Type | Degrees of Freedom (A) or Source (B) |
|---|---|---|
| 1) Repeated measurements | 0.0005 K (A) | DF = 1785 |
| 2) Temperature determination<br>- PRT calibration<br>- Regression analysis<br>- Resistance measurement | <br>0.005 K (B)<br>0.0052 K (A)<br>0.055 K (B) | <br>NIST Calibration<br>DF = 15<br>$u(\Delta T_{2C}) = a/\sqrt{3}$ |

***Combined Standard Uncertainty for λ Measurement***

Rearranging eq (2) in the text and applying the error propagation formula, the standard uncertainty for measured values of λ was evaluated with the following equation:

$$u_c^2(\lambda) = c_Q^2 u_c^2(Q) + c_A^2 u_c^2(A) + c_L^2 u_c^2(L) + c_{\Delta T}^2 u_c^2(\Delta T), \qquad \textbf{(B-15)}$$

where

$c_Q = \partial\lambda/\partial Q = L/(A\Delta T)$,
$c_A = \partial\lambda/\partial A = -(QL)/(A^2\Delta T)$,
$c_L = \partial\lambda/\partial L = Q/(A\Delta T)$, and
$c_{\Delta T} = \partial\lambda/\partial\Delta T = -(QL)/(A\Delta T^2)$.

The individual standard uncertainties for the specimen heat flow ($Q$), meter area ($A$), in-situ thickness ($L$), and specimen temperature difference, ($\Delta T$) were determined as described above.

Table B-6 summarizes the input quantities, $X_i$, estimates, $x_i$, standard uncertainties, $u_i$, and sensitivity coefficients, $c_i$, for $Q$, $A$, $L$, and $\Delta T$. The combined standard uncertainty, $u_c$, for λ was 0.00020 W/(m⋅K) (relative standard uncertainty of 0.57 percent).

**Table B-6**
**Combined Standard Uncertainty (k=1) for Thermal Conductivity Measurement**

| **Quantity, $X_i$** | **Estimate, $x_i$** | **u($x_i$)** | **Sensitivity Coefficients, $c_i$** | **Uncertainty (W/(m⋅K))** |
|---|---|---|---|---|
| Q | 3.5665 W | 0.0101 W | $9.76\times10^{-3}$ $m^{-1}K^{-1}$ | 0.00010 |
| A | 0.1297 $m^2$ | $4.18\times10^{-5}$ $m^2$ | -0.269 $Wm^{-3}K^{-1}$ | 0.00001 |
| L | 0.02533 m | $9.10\times10^{-5}$ m | 1.375 $Wm^{-2}K^{-1}$ | 0.00013 |
| ΔT | 20.00 K | 0.067 K | $-1.74\times10^{-3}$ $Wm^{-1}K^{-2}$ | 0.00012 |
| λ | 0.0348 W/(m·K) | | **Total** | 0.00020 |

***Mean Temperature (T)***

The mean temperature was determined from eq (B-16)

$$T = \tfrac{1}{2}(T_h + T_c) = \tfrac{1}{2}\left(T_h + \tfrac{1}{2}(T_{c_1} + T_{c_2})\right). \qquad \textbf{(B-16)}$$

The combined standard uncertainty of $T$ was 0.034 K.

## Appendix C

### Uncertainty Analysis for Bulk Density (ρ)

The Type A and Type B standard uncertainties for the determination of bulk density for the meter area are summarized in Table C-1. The Type A standard uncertainties for the length measurements were computed by pooling the standard deviations from a relatively small number of measurements for each specimen. The Type B standard uncertainties for the length measurements were assumed to have a uniform distribution in the interval 2*a*, where *a* was the smallest length interval of the steel rule or calipers. The interval 2*a* for the steel rule and calipers was 0.5 mm and 0.1 mm, respectively.

**Table C-1**
**Uncertainty Budget: Meter Area Bulk Density (ρ)**

| Source of Uncertainty | Standard Uncertainty $u(x_i)$ and Type | Degrees of Freedom (A) or Source (B) |
|---|---|---|
| 1) Calibration of scale (m) | 0.1 g (B) | Manufacturer Specification (k=1) |
| 2) Diameter measurement (d):<br>- repeated measurements<br>- uncertainty of steel rule | <br>0.31 mm (A)<br>0.29 mm (B) | <br>DF = 30<br>$u(d_2) = a/\sqrt{3}$ |
| 3) Thickness measurement (L):<br>- repeated measurements<br>- uncertainty of calipers<br>- uncertainty of flat table | <br>0.082 mm (A)<br>0.058 mm (B)<br>0.015 mm (B) | <br>DF = 120<br>$u(L_2) = a/\sqrt{3}$<br>Manufacturer Specification (k=1) |

The combined standard uncertainty $u_c^2(\rho)$ was determined using the standard uncertainties given in Table C-1 and the following equation:

$$u_c^2(\rho) = c_m^2 u^2(m) + c_d^2[u^2(d_1) + u^2(d_2)] + c_L^2[u^2(L_1) + u^2(L_2) + u^2(L_3)], \qquad \textbf{(C-1)}$$

where $c_m$, $c_d$, and $c_L$ were 308.6, -783.1, and -6409, respectively, and were determined from eq (B-3) and eq (3) in the text. The combined standard uncertainty $u_c(\rho)$ for the meter area bulk density determination was 0.72 kg/m$^3$. The relative standard uncertainty for the grand average of 159.6 kg/m$^3$ was 0.45 percent.